Biomaterials Advances 154 (2023) 213655

Contents lists available at ScienceDirect

Biomaterials Advances

journal homepage: www.journals.elsevier.com/materials-science-and-engineering-c

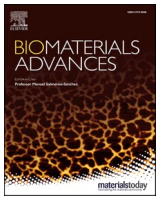

Review

Advancements in tailoring PEDOT: PSS properties for bioelectronic applications: A comprehensive review

Miriam Seiti [a], Antonella Giuri [b], Carola Esposito Corcione [c], Eleonora Ferraris [a,*]

[a] Department of Mechanical Engineering, KU Leuven, KU Leuven Campus De Nayer, Jan De Nayerlaan 5, Sint-Katelijne-Waver 2860, Belgium
[b] CNR-NANOTEC-Istituto di Nanotecnologia, Polo di Nanotecnologia, c/o Campus Ecotekne, via Monteroni, I-73100 Lecce, Italy
[c] Università del Salento, via per Monteroni, km 1, I-73100 Lecce, Italy

ARTICLE INFO

Keywords:
Review
PEDOT:PSS
Bioelectronics
Biological interfaces
Carbon fillers

ABSTRACT

In the field of bioelectronics, the demand for biocompatible, stable, and electroactive materials for functional biological interfaces, sensors, and stimulators, is drastically increasing. Conductive polymers (CPs) are synthetic materials, which are gaining increasing interest mainly due to their outstanding electrical, chemical, mechanical, and optical properties. Since its discovery in the late 1980s, the CP Poly(3,4-ethylenedioxythiophene):poly (styrene sulfonic acid) (PEDOT:PSS) has become extremely attractive, being considered as one of the most capable organic electrode materials for several bioelectronic applications in the field of tissue engineering and regenerative medicine. Main examples refer to thin, flexible films, electrodes, hydrogels, scaffolds, and biosensors. Within this context, the authors contend that PEDOT:PSS properties should be customized to encompass: i) biocompatibility, ii) conductivity, iii) stability in wet environment, iv) adhesion to the substrate, and, when necessary, v) (bio-)degradability. However, consolidating all these properties into a single functional solution is not always straightforward. Therefore, the objective of this review paper is to present various methods for acquiring and improving PEDOT:PSS properties, with the primary focus on ensuring its biocompatibility, and simultaneously addressing the other functional features. The last section highlights a collection of designated studies, with a particular emphasis on PEDOT:PSS/carbon filler composites due to their exceptional characteristics.

1. Introduction

The field of bioelectronics is rapidly expanding, and the demand for biocompatible, stable, and electroactive materials for robust biological interfaces, with electronic sensors and stimulators, is increasing. In this scenario, conductive polymers (CPs) have become extremely attractive as electrochemical bioengineered sensors for tissue engineering (TE), drug delivery and regenerative medicine [1]. Particularly, CPs can be used for electrophysiology recording and/or stimulation of biological cellular activities (e.g. cardiac or neural cultures) [2], biomolecules interfaces [3], electronic soft-skin sensors [4], bioactuators [5], drug delivery systems [6], and organic-electronic ion-pumps [7]. CPs are synthetic materials composed of organic macromolecules, which gained high interest due to their outstanding electrical properties. They are able to merge the advantages of semiconductors or metals, such as π-conjugated backbones and optical properties, along with the superior processability and mechanical properties of conventional organic polymers [8,9]. Among the CPs, the most used are: Polypyrrole (PPy), Polythiophene (PT), Polyacetylene (PA) and Polyaniline (PANI) [10]. Besides, in the last years, more attention raised for a specific electroactive polymer in the family of Polyheterocycles, that is Poly(3,4-ethylenedioxythiophene):poly(styrenesulfonic acid) (PEDOT:PSS) [11].

PEDOT:PSS has been reported for the first time in the scientific community in 1997, when poly(3,4-ethylenedioxythiophene) (PEDOT) was developed from the EDOT monomer as a new polythiophene (PT) derivative at the Bayer AG laboratories (Germany). PEDOT reveals high values of conductivity (S, [S/m]), $S \sim 300$ S/cm, excellent stability in the oxidized state, and transparency in thin films [12,13]. However, its insolubility and instability (conventionally in water) requires a doping process, usually performed with the addition of a counterion to the PEDOT backbone. Among different options (synthetic or biological-based), the water-soluble polyelectrolyte poly(styrene sulfonic acid) (PSS) has become the most used counterion in water-based dispersions. PSS is a polyanion generally recognized to act as a p-type doping counter

* Corresponding author.
E-mail address: eleonora.ferraris@kuleuven.be (E. Ferraris).

https://doi.org/10.1016/j.bioadv.2023.213655
Received 2 June 2023; Received in revised form 22 September 2023; Accepted 6 October 2023
Available online 10 October 2023

ion for charge-balancing during polymerization, hence it consents hole mobility in the PEDOT conjugated backbone, enhancing its dispersion in polar solvents (like water) [14]. As reported by Lu et al. [15], three main molecular interactions indeed occur in PEDOT:PSS: i) electrostatic attractive forces between $PEDOT^+$ and PSS^- chains, ii) noncovalent interactions (π-π stacking) of PEDOT adjacent chains, and iii) interchain entanglements between long PSS chains. The PEDOT/PSS ratio also greatly influences the conductivity of the polymer, making it adaptable to different applications, as a p-type or electrode. Particularly, the most used nanosuspension formulation of PEDOT:PSS contains aggregates of PEDOT:PSS nanoparticles in the range of [0.5–0.6] μm [16], with an excess of PSS in a PEDOT/PSS weight ratio of 1/2.5 [17]. Nowadays, PEDOT:PSS is commercially distributed in powder form or as a blue colour aqueous dispersion, mainly by Heraeus Holding GmbH (Clevios™) [18] and Agfa-Gevaert N.V. (Orgacon™) [19].

PEDOT:PSS is an easy, processable, and environmental friendly CP, composed of conductive π-conjugated $PEDOT^+$ and insulating PSS^- charged colloidal particles [20]. It is well-recognized as a doped p-type semiconductor [21] due to its cost-effective fabrication, water-solubility, good chemical and physical stability, tunable conductivity, good biocompatibility, excellent thermal stability, and high visible light transmittance (transparency) [17,22],. Thus, PEDOT:PSS is considered as one of the most capable organic electrode materials in the field of electronics to replace conventional carbon, metal (Au, Cu, Pt, etc.) or conductive glass based electrodes. It is indeed able to promote direct electron transfer at a fraction of cost, and low process temperatures [22]. For instance, PEDOT:PSS can be a promising substitute of the conductive glass indium tin oxide (ITO, S ~ 3000–6000 S/cm on glass [23]), which is the conventional material used for the fabrication of transparent electrodes. Indeed, resources of indium on earth are strictly limited and its fabrication is far from being cost-effective [23]. Besides, its brittle behavior is not ideal for producing novel flexible and stretchable electronics. The same enunciation is also valid for platinum and gold: a Young's modulus in the order to tens to hundreds GPa is not ideal and compatible with most of soft biological tissues [24].

The easy deposition, especially from a liquid state, is another interesting aspect of PEDOT:PSS based materials. In the last years, several film/coating forming have been adopted for the fabrication of thin films/electrodes [8]. In the following paragraph, an explanation of the primary production techniques is provided for PEDOT:PSS structures used in this review. However, for a more comprehensive overview of coating techniques, we recommend referring to these referenced reports [8,25].

PEDOT:PSS film fabrication has undergone by means of various coating techniques, such as dip coating, drop coating, and spray coating, among others. Dip coating and drop coating stand out as the simplest and most scalable approaches for generating a PEDOT:PSS film on free-form substrates. In the case of dip coating, it involves immersing a chosen substrate into liquid PEDOT:PSS for a specified duration at a controlled rate, while drop coating entails applying PEDOT:PSS droplets onto the substrate surface. Subsequently, the solvents within the solution evaporate, and the material undergoes drying. However, it is worth noting that it is challenging to achieve uniform coating distribution in both approaches, and precise control over film thickness is elusive. Alternatively, spin-coating stands as one of the most popular coating methods, due to its capacity to swiftly produce consistent, and replicable nanoscale thin films. In this technique, liquid PEDOT:PSS is dropped at the center of a substrate, which is placed on a rotating platform, set to a particular speed and acceleration. The material is then spread radially outward due to centrifugal forces until a thin film is formed. The primary drawback here lies in the excess material that goes to waste and in an irregular thickness at the edges [26]. Spray coating also offers a cost-effective approach, particularly in the coating of large area thin films over irregular surfaces. In this process, the PEDOT:PSS solution is sprayed onto the surface of the substrate using a nozzle positioned at a precise distance from the substrate itself. This results in a smooth coating, however, it may come with challenges related to surface wettability, because of adhesion on the substrate, which is however a common aspect in all techniques and can be solved via surface activation.

Printing technologies, such as screen printing and inkjet printing, offer intriguing alternatives to traditional coating techniques, such as inkjet printing, screen printing, aerosol jet printing, and roll-to-roll techniques [27–29]. Specifically, screen printing is an economically viable and scalable deposition method, where the PEDOT:PSS ink is pushed through a stencil onto a predefined pattern on the substrate, minimizing ink wastage. On the other hand, inkjet printing, whether continuous inkjet or drop-on-demand inkjet, represents a widely embraced direct writing technology. In this process, liquid ink is precisely dispensed in the form of microdroplets via an array of fine nozzles onto the substrate.

In any technique, control over the evaporation rate of the solvent due to annealing temperature, time, and humidity conditions, is necessary in order to obtain a homogenous film formation from randomly oriented PEDOT crystals surrounded by hydrophilic PSS chains in the aqueous dispersion [30]. Also, it must be taken into account the performance of the selected technique in biologically relevant conditions. This means ensuring that the selected technique does not compromise the stability of compounds or their ability to degrade, which may cause the release of cytotoxic compounds in the medium culture.

Due to this wide portfolio of techniques, PEDOT:PSS thin films and electrodes have been fine-tuned for a wide range of applications in the field of organic electronic devices, including flexible electronics [31], conductive coatings [32], super capacitors [33,34], electrochemical sensors [35], organic electrochemical transistors (OECTs) [21,36], energy harvesting thermoelectric (TEs) devices [37,38], optoelectronic devices [14,23,26,39–46], etc. Furthermore, PEDOT:PSS has been utilized in different forms, such as electrode coating, active film or electrode, and scaffold [47] for the control over cellular activity in two dimensional (2D) and three dimensional (3D) soft, stretchable, (porous) biological interfaces [48].

Despite the outstanding properties and flexible use of such material, it took almost 2 decades for PEDOT:PSS to be truly appreciated among the scientific community. In this regard it is worth noting the number of publications on the use of PEDOT:PSS increased up to ~1000/year just in the last four years, as shown in Fig. 1. Particularly, in the period 1997–2022, 11,782 records were counted by Scopus (keyword "PEDOT:PSS"), among which almost 90 % are journal articles, which around 50 % reside in the category Materials Science Multidisciplinary. Articles with PEDOT:PSS implemented in bioelectronics and/or biocompatible applications date back to 2005, but only recently they have undergone an increase, with >50 publications/year in the last three years, for a total of 210 and 178 publications found with the keywords "Bioelectronic(s) PEDOT:PSS", and "Biocompatible PEDOT:PSS", respectively (see Fig. 1). In both cases, >88 % are journal articles, among which >40 % lie in *Materials Science Multidisciplinary*. Overall, it is evident an increasing interest of PEDOT:PSS for bioelectronics, which is expected to growth even more in the near future.

In bioelectronics, the need to converge the conductive properties of metal electrodes with biocompatible, soft, engineered hydrogels is crucial to obtain a functional biological interface [48]. Multiple challenges are faced in this context. Firstly, the final construct must be biocompatible when in contact with the targeted cellular entity. Secondly, the PSS doping process is known to affect the oxidation level and electronic properties of PEDOT [49], causing a decrease in the PEDOT:PSS electrical conductivity. Numerous studies focused on the enhancement of PEDOT:PSS conductivity through a so called '*secondary doping*', however, few solutions can be adopted to obtain biocompatible PEDOT:PSS constructs. Thirdly, most of the bio-electrochemical interfaces require high stability in physiological or aqueous solutions and adhesion to the selected substrate. In each challenge, the selection of appropriate not-cytotoxic chemical compounds is necessary.

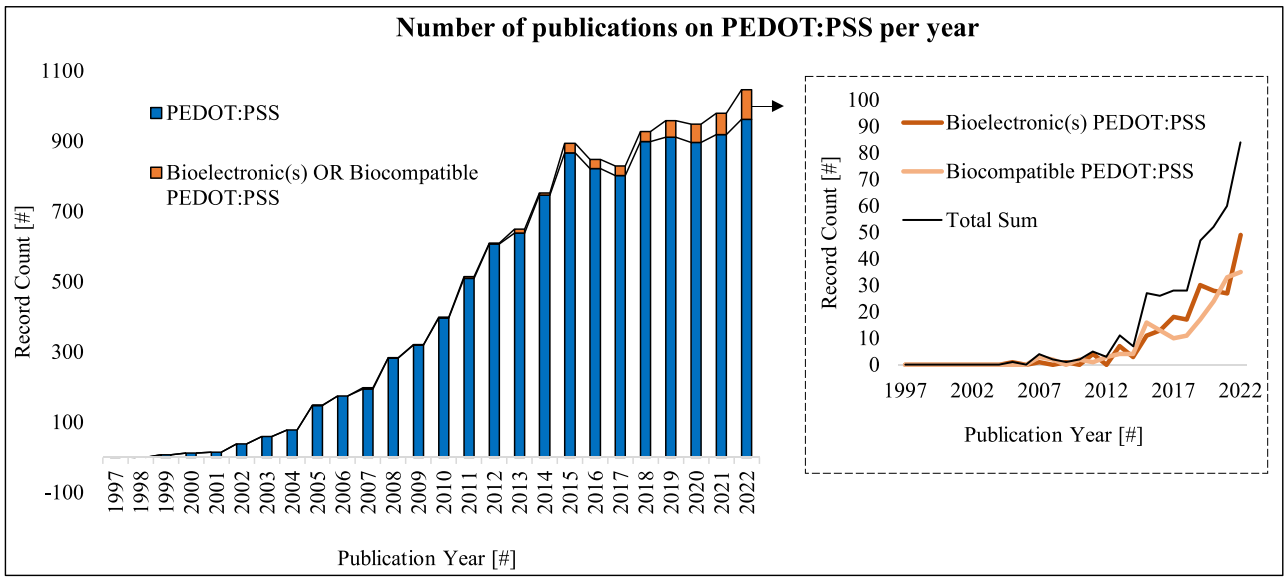

Fig. 1. PEDOT:PSS in the scientific community: number of publications per year in the range 1997–2022, showing a positive growing trend. Data were acquired from Scopus, with the following keywords: i) PEDOT:PSS, ii) Bioelectronic(s) PEDOT:PSS, and iii) Biocompatible PEDOT:PSS.

Tailoring PEDOT:PSS properties for bioelectronics can be then circumscribed into five main requirements: i) biocompatibility, ii) conductivity, iii) stability in saline solution, iv) adhesion to the substrate, and v) potential (bio)-degradability. Fig. 2 summarizes the chemical-physical properties of PEDOT:PSS for bioelectronic applications and the various treatments described in the manuscript.

This paper aims to present a selection of different methods applied to enhance PEDOT:PSS conductivity, stability, and adhesion in water-based solution, simultaneously ensuring its biocompatibility for bioelectronic applications. Each section is divided based on the challenge pursued. *Section 2* illustrates tailoring the chemical-physical properties of PEDOT:PSS to enhance its conductivity, mostly with organic dopant agents. *Section 3* considers methods to increase PEDOT:PSS chemical stability in aqueous solutions and adhesion to the substrate. *Section 4* discusses methods to increase its biocompatibility whereas *Section 5* proposes an observation concerning the concept of biodegradability. *Section 6* is dedicated to the description of conductivity and biocompatibility enhancement approaches by means of the addition of carbon fillers. This section also presents a portfolio of bioelectrical applications collected from the recent literature, in order to offer a general overview of the achieved progresses as inspiration for future research. Ultimately, the conclusions, along with future perspectives, are presented to summarize the key concepts discussed.

2. Tailoring PEDOT:PSS electrical conductivity

Pristine PEDOT:PSS is known to own high electrical stability, with no change under thermal treatment in air over 1000 h at 100 °C, and a variable electrical conductivity depending on the ratio PEDOT/PSS, with values in the range of $S = [10^{-5} - 1]$ S/cm [51,52], as reported in Table 1. This is mainly caused by an excess of insulating PSS chains in the PEDOT:PSS structure, which restraints conductive PEDOT chains.

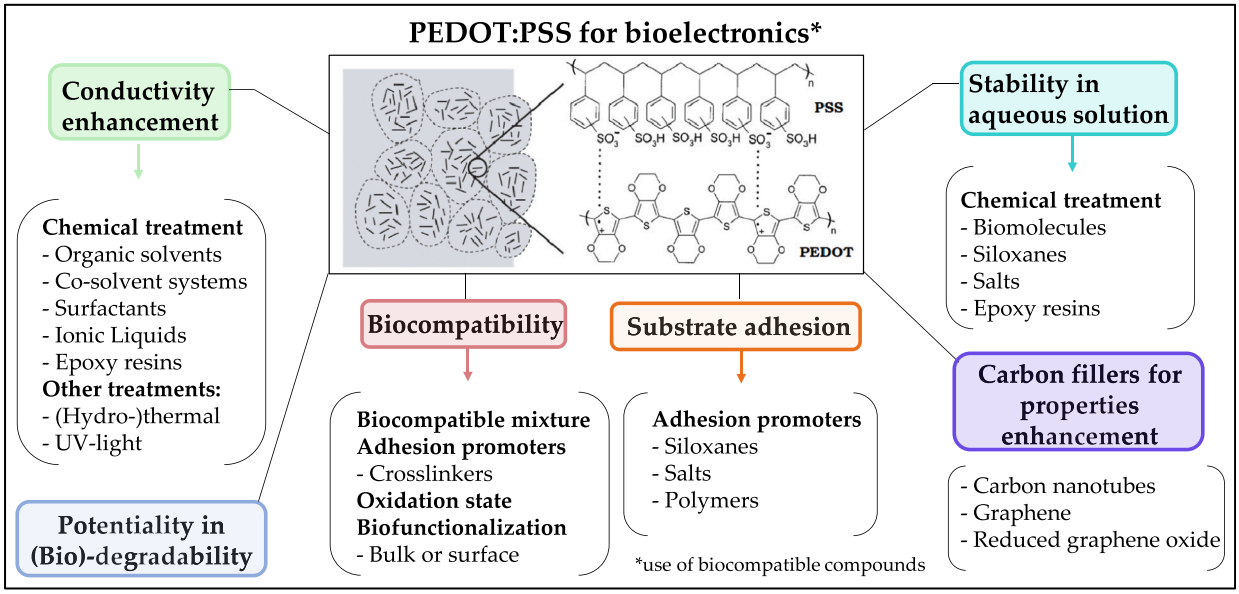

Fig. 2. Introduction to PEDOT:PSS: chemical formula of PEDOT:PSS, with main PEDOT:PSS chemical-physical properties for bioelectronic applications. Cartoon of PEDOT:PSS chemical structure republished with permission from M. M de Kok [50], Copyright© © 2004 WILEY-VCH Verlag GmbH & Co. KGaA, Weinheim.

Table 1
Chemical and physical properties of the commercial PEDOT:PSS aqueous dispersion. Data taken from Fan et al. [53] and Elschner et al. [54].

PEDOT:PSS	PEDOT/PSS ratio (by weight)	Solid content (%)	Viscosity [cP at 20 °C]	Particle Size distribution	Conductivity (S/cm)	Resistivity [Ω cm]
Clevios™ P VP AI4083	1:6	1.3–1.7	5–12	D_{50} = 80 nm D_{90} = 100 nm	10^{-3}	500–5000
Clevios™ PVP CH8000	1:20	2.4–3.0	2–20	D_{50} = 35 nm D_{90} = 50 nm	10^{-5}	10^4–3 × 10^5
Clevios™ P	1:2.5	1.3	80	D_{50} = 80 nm	<10	500–5000
Clevios™ HTL Solar	1:2.5	1.0–1.3	8–30	n.a.	0.1–1	n.a.
Clevios™ PH500	1:2.5	1.0–1.3	8–25	D_{50} = 30 nm	300–500[a]	n.a.
Clevios™ PH750	1:2.5	1.0–1.3	8–25	D_{50} = 30 nm	750[a]	n.a.
Clevios™ PH1000	1:2.5	1.0–1.3	15–50	D_{50} = 30 nm	850–1000[a]	<0.0012[a]

[a] For dispersion containing 5 % of Dimethyl sulfoxide (DMSO).

Therefore, it is necessary to increase *S* in order to use PEDOT:PSS as a conductive electrode/interface.

Jeong et al. [55] demonstrated that the conductivity of PEDOT:PSS films can be increased up to $S = 125.367$ S/cm, by means of a hydrothermal treatment which employs the use of water at a relative humidity >80 %, and heating temperatures higher than 61 °C. This green-friendly and cost-effective method can be directly performed by means of an autoclave, which also ensures sterilization for cell culturing. However, more efficient methods to increase *S* have been discovered during the last decade, such as the doping process. As explained by Huseynova et al. [9], doping can induce an increase in the concentration of mobile charge carriers, allowing a higher conduction all over the polymer backbone and a neutralization of some PSS^-. This mechanism is known as *secondary doping*, since the first type of doping, of p-type nature, is achieved between PEDOT and PSS and it generates a conductive PEDOT:PSS structure with stable ionic bonds between $PEDOT^+$ and PSS^- chains [9]. The secondary doping can be applied in both pre- and post-treatments: pre-treatments (or direct addition) are used prior the film formation process, while post-treatments are employed on the annealed film. In the case of thin films, these processes are also known to affect the film transmittance, morphology, roughness, and thickness [9]. For instance, Rivnay et al. [56] found out that if PEDOT:PSS (Clevios™ PH-1000) thin films are modified with specific co-solvents, such as ethylene glycol (0.0–50.0 v/v%) and 4-Dodecylbenzenesulfonic acid (DBSA) (0.002 v/v %), morphological and structural re-arrangements occur and induce an effect on the control of PEDOT:PSS electronic and ionic mobilities.

Secondary doping treatments include chemical- (most common one), thermal-, or light-based process [1]. Particularly, effective chemical approaches include organic solvents, surfactants, ionic liquids, salts, carboxylic, inorganic acids, salt zwitterion, or acid/alkai treatments [57,58]. As an example, Xia et al. [59] obtained PEDOT:PSS films with a conductivity increase from $S = 0.3$ S/cm to $S = 1325$ S/cm, via a fluoro compound hexafluoroacetone (HFA) treatment for four consecutive times. The highest PEDOT:PSS conductivity reported ($S \sim 4380$ S/cm, almost comparable to the ITO's one) has been instead achieved via a controlled sulfuric acid (H_2SO_4) post-treatment, which induces the formation of crystallized PEDOT:PSS nanofibrils by PSS removal via charge-separation [60]. Despite these successful results, the two approaches cannot be used in bioelectronics, due to their cytotoxic or corrosive nature [21]. Also, commercial PEDOT:PSS solutions which are custom made for PE cannot usually be exploited due to the presence of cytotoxic solvents, like diethylene glycol [61].

So far, the use of organic solvents is the most accepted method in bioelectronics, due to the possibility to enhance the conductivity of PEDOT:PSS commercial aqueous dispersions from 0.2 to >100 S/cm by the easy addition of i) a polar organic solvent with a high boiling point (b.p.), or ii) a co-solvent system of water mixed with an organic solvent with a low b.p [62].. In the first case, a conformal change of PEDOT chains from a coil to an expanded linear structure occurs, which promotes the inter-PEDOT chain change transport [57,58,62] and, as a consequence, an increase in *S* by a few orders of magnitude [63]. This phenomenon is caused by a phase separation between $PEDOT^+$ and PSS^- chains. Particularly, polar co-solvents donate protons (H^+), thus a removal of PSS^- chains (SO^{-3}) produces PSS-H^+ and a reduction in coulomb interaction [64]. For this reason, the presence of water in the dispersion does not contribute to the S enhancement [62]. Besides, the higher is the b.p. of the co-solvent used, the more is the time left for a morphological rearrangement of the polymer chains, resulting in a higher decrease in electrical resistance between dried particles [64]. Co-solvent addition can be performed by means of pre- or post-treatments, such as in the case of ionic liquids and anionic surfactants. Particularly, post-treatments are film dipping (immersion) in the solvent, solvent dropping on the film, polar solvent vapor annealing of the film, or film spin/spray rinsing [9].

In the following paragraphs, a list of representative studies on the use of polar organic solvents in PEDOT:PSS dispersions is presented.

- *Dimethyl sulfoxide (DMSO)*. Dimethyl sulfoxide molecule is a pyramidal structure with sulfur, oxygen, and carbon atoms on the corners. The sulfur-oxygen bond is fairly polar so that the liquid has a high dielectric constant. The presence of a liquid structure and association forces is reflected in a high freezing point, a low entropy of fusion, a high boiling point, and a high entropy of vaporization [65]. DMSO is an aprotic solvent that has incited considerable debate in the scientific and academic world. It is soluble in both water and therapeutic, toxic agents that are not soluble in water. All these properties have suggested its possible applications in different fields, such as CPs. For instance, Lu et al. [15] developed conductive PEDOT:PSS (Clevios™ PH1000) nanofibrils hydrogels, with the addition of DMSO (13.0 v/v%) as second dopant. Specifically, the mixture was spin-casted, dry annealed x3 times (130 °C for 30 min), and rehydrated. During the dry annealing process, a densification of PEDOT:PSS, with subsequent recrystallization of PEDOT-rich nanofibrils and rearrangement of PEDOT and PSS chains, was observed. In wet physiological conditions, the hydrogel showed a conductivity $S \sim 20$ S/cm, a stretchability over 35 %, and low Young's modulus ~2 MPa. A higher conductivity improvement from $S = 0.07$ S/cm to $S = 73$ S/cm was instead achieved by Cruz-Cruz et al. [66], by doping PEDOT:PSS (Baytron) films with a DMSO concentration of 17.0 w/w % (see Fig. 3A). In this case, the cause of conductivity enhancement was mostly linked to the reduction of the PSS barrier between PEDOT grains, allowing an increase of their size. Alternatively, Kim et al. [68] used PEDOT:PSS (Sigma Aldrich) at an amount of 2.2–2.6 w/w % in an aqueous suspension with DMSO (2.0 w/w%), to fabricate nano-arches-like structures with 400 nm radius and $S = 200$ S/cm (see Fig. 3B). The structures combined high stretchability with good electronic performances, useful for bioelectronic photo-switches, or electrochemical transistors. Post-treatments of PEDOT:PSS film with an exposure to DMSO vapor, have been also used as alternative methods to control film formation and conductivity increase over the exposure time, due to a conformational change of swelling interconnected polymer chains [69,70].

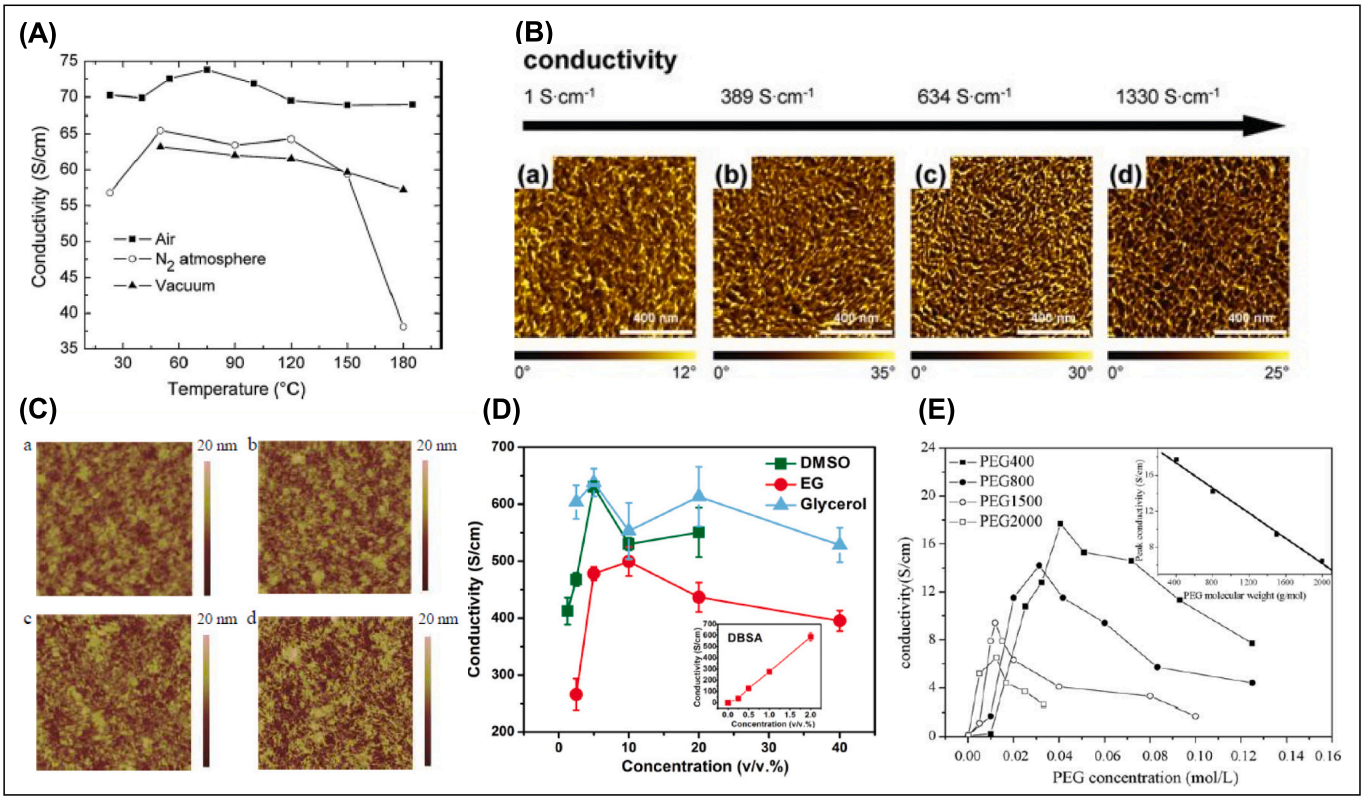

Fig. 3. Tailoring PEDOT:PSS for electrical conductivity enhancement: representative cases using biocompatible compounds. (A) Conductivity of PEDOT:PSS thin films doped with DMSO as a function of annealing temperature in air, N_2, or vacuum atmosphere. Republished with permission from Cruz-Cruz et al. [66], Copyright© Elsevier B.V. 2010. (B) AFM images of PEDOT:PSS thin films (Clevios™ PH1000) before and after conductivity doping: PEDOT:PSS as (a) pristine, (b) 5.0 v/v% of DMSO dopant, (c) 6.0 v/v% of EG dopant, and (d) solvent post-treated, 6.0 v/v% of EG dopant. Republished with permission from Kim et al. [67], Copyright© Wiley 2011. (C) PEDOT:PSS electrodes (Clevios™ PH1000) as (a) pristine, (b, c, d) with 1.0, 6.0, and 9.0 v/v%, of EG dopant, respectively. Republished with permission from Cui et al. [40], Copyright© Springer Nature 2019. (D) Effect of co-solvents concentration of DMSO, EG, and glycerol on PEDOT:PSS films (Clevios™ PH1000, thickness ca. 150 nm). Republished with permission from Zhang et al. [21], Copyright© AIP Publishing 2015; (E) Surfactants effect on PEDOT:PSS (Bayer AG) films' conductivity: PEG influence on S at different M_w. Republished with permission from Wang et al. [52], Copyright© Elsevier B.V. 2005.

- *Ethylene glycol (EG)*. Ethylene glycol is the simplest diol and has various exceptional properties due to its typical structure (i.e., two hydroxyl (OH) groups at adjacent positions along a hydrocarbon chain). It is a colorless, odorless, relatively non-volatile, and hygroscopic liquid with low viscosity. Indeed, owing to its unique properties, it is proposed in a significant number of industrial applications (e.g. energy, plastics, automobiles, and chemicals) [71]. Cui et al. [40] studied the effect of EG (1.0–9.0 vol%) as conductivity enhancer in a PEDOT:PSS (Clevios™ PH1000 and P VP AI 4083) water-based dispersions. The most promising films were achieved at a EG 6.0 vol %, displaying a transmittance of 96 % at $\lambda = 550$ nm and a uniform low root-mean-square (RMS) roughness of 1.83 nm (see Fig. 3C). This favoured the phase separation of the PEDOT:PSS chains, thus increasing the sheet resistance (R_{sh}, [Ω/sq]) up to $R_{sh} = 195$ Ω/sq. At the same EG concentration, S can be also further enhanced by a post-treatment in an EG bath for 30 min. Post-treated PEDOT:PSS (Clevios™ PH 1000) films by Kim et al. [67] indeed showed an increase in conductivity till $S = 1418$ S/cm, due to a combined action of PSS chains depletion and PEDOT-rich grains stretching orientation, which generate a more compact structure and larger contact areas, respectively. Likewise, Stříteský et al. [72] spin-coated different PEDOT:PSS ink-jet printing inks (particularly Sigma Aldrich n. 483 095 and PEDOT/PSS-AS) and demonstrated that a combined post-treatment by EG and subsequent thermal annealing could reduce their electrical resistance (R, [Ω]) of 2 orders of magnitude.
- *Glycerol*. Glycerol is a naturally occurring 3-carbon alcohol in the human body. It is the simplest triol, characterized by structural backbone of triacylglycerol molecule. It can be found in all natural fats and oils as fatty esters and is an important intermediate in the metabolism of living organisms. It is totally miscible with water and many alcohols, but also with many heterocyclic compounds. A significant and increasing resource of glycerol is as a byproduct in the production of biodiesel. Glycerol is currently used in a wide variety of applications due to its specific combination of chemical and physical properties and its physiological innocuity [73]. Particularly, it has been used to increase the PEDOT:PSS electrical conductivity for electric charge transport, up to a certain concentration, due to a decrease of energy barrier and a structural reorientation of PEDOT:PSS chains [74,75]. Garma et al. [76] used 10.0 w/w% of glycerol in a waterborne PEDOT:PSS solution (0.6–1.2 wt%, Clevios™ PJet 700) in order to produce contact pads, feed lines, and electrodes for microelectrode arrays (MEAs). The impedance (Z, [Ω]) of these devices had an average value of $Z = 19.50$ kΩ at 1 kHz, which was far below the value of the respective used MEAs with flat gold electrodes, equal to $Z = 160$ kΩ. Tsukada et al. [77] electrochemically combined PEDOT:PSS (Clevios™ P) with glycerol and silk fiber bundles in order to obtain microfiber reinforced composites ($S = 0.102$ S/cm). Similarly, Zhang et al. [21] used mixtures containing a PEDOT:PSS aqueous suspension (1.1 w/w%, Clevios™ PH1000) with the surfactant DBSA (0.5 v/v%) and glycerol (5.0 v/v%) to produce PEDOT:PSS films with a final S = 600–700 S/cm (see Fig. 3D).
- *4-Dodecylbenzenesulfonic acid (DBSA)*. 4-Dodecylbenzenesulfonic acid is an alkyl sulfonate. It participates in the preparation of a polymer along with polystyrene-*block*-poly(4-vinylpyridine) and a *comb*-coil A-*block*-(B-*graft*-C) type of copolymer. It can be used for

several applications, such as: solvent for the synthesis of 2-(1,5-diaryl-1,4-pentadien-3-ylidene)-hydrazinecarboximidamide hydrochlorides; in-situ coating of rutile nanoparticles; stabilizer in the preparation of colloidal suspensions; fabrication of solid-state dye-sensitized solar cells (DSSCs) [78]. In combination with PEDOT:PSS (Clevios™ PH-1000), DBSA (0.5 w/w%) has been used by Inal et al. [79] for the fabrication of ice-templated PEDOT:PSS scaffolds, which also included collagen (0.05 w/w%, type I from rat tail) and 3-glycidoxypropyltrimethoxysilane (GOPS) (3 w/w%) as crosslinker/stabilizer for the co-culturing of fibroblasts and epithelial cellular lineages.

Alternatively, a co-solvent system with water is needed in the use of organic solvents at low b.p., in order to actuate a phase segregation between $PEDOT^+$ and PSS^-, which eventually leads to a partial removal of PSS^- [62]. By testing several compounds at low b.p., such as Ethanol (EtOH), Methanol (MeOH), Isopropanol (IPA) or Acetone at 0.0–20.0–40.0–60.0–80.0–100.0 v/v%, Xia et al. [62] demonstrated that the conductivity of PEDOT:PSS (Clevios™ P) did not change remarkably when the solvent was directly added into the aqueous dispersion, contrary to a co-solvent system [62]. Moreover, S was also positively influenced by the volume fraction in the co-solvent, the dielectric constant (EtOH generally rose more than IPA, which has a lower dielectric constant), and the treating temperature (range [120–180] °C). The authors also demonstrated that the presence of OH groups did not contribute in the conductivity enhancement, in accordance with other studies [58].

Biocompatible surfactant treatments can be also applied to increase S in PEDOT:PSS. For instance, Wang et al. [52] investigated the addition of the biocompatible polymer polyethylene glycol (PEG) at different molecular weights (Mw) (Mw_{PEG} = 400, 800, 1500, 2000) in PEDOT:PSS (Bayer AG) aqueous dispersions for thin films (thickness ca. 30–50 nm). Interestingly, the authors demonstrated that the most favorable concentration of PEG for an increase in S was inversely proportional to the Mw_{PEG}. The sharpest pick in S was indeed observed using the lowest Mw_{PEG} = 400, at a concentration of 0.04 mol/L, S = 17.7 S/cm. A gradual decrease in S was also detected with a further addition of the surfactant. Instead, in the case of higher values of Mw, like Mw_{PEG} = 2000, the highest values of S were reached at very low concentrations, such as 0.01 mol/L (see Fig. 3E). The authors hypothesized that PEG may weaken the electrostatic interaction between PEDOT and the excessive PSS, by forming hydrogen bonds with the PSSH sulfonic groups, thus allowing a more expanse PEDOT chains conformation. Soleimani-Gorgani et al. [64] also investigated the effect of PEG (Mw_{PEG} = 200) in PEDOT:PSS aqueous dispersion (Sigma-Aldrich, 1.3 w/w%). Specifically, the particle size of PEDOT:PSS, which has a usual diameter of ca. tens nanometer, was detected higher with an increase in the Mw_{PEG}, mostly due to the enlargement in space between the $PEDOT^+$ and PSS^- chains. This effect was also verified via atomic force microscopy (AFM), where a change in the roughness morphology of PEDOT:PSS was detected from 2.9 to 3.55 nm at RMS. Li et al. [80] also examined the addition of PEG (Mw_{PEG} = 200, 400, 1500) at 1.0, 2.0, and 4.0 v/v% for PEG_{400} and at 4.0 v/v% for the others, in PEDOT:PSS aqueous suspension (Clevios™ PH1000) to study an interesting mechanism of autonomic self-healing. It was found that PEG could indeed induce a change in the mechanical properties of pristine PEDOT:PSS, favouring a lower elastic modulus and an increase in the elongation at break. This phenomenon is likely to be caused by a material flowing back to the damaged area after cutting, and it is more significant in low Mws_{PEG} at high concentrations, due to a higher mobility of molecular chains. Such kind of mechanism may be very useful for the fabrication of wearable bioelectronic devices.

Biocompatible ionic liquids, like organic or inorganic salts, are also another valuable alternative to organic solvents, with the main difference of not being volatile [57]. Liu et al. [81] used a PEDOT:PSS aqueous suspension (Clevios™ PH1000, 1.0–1.3 w/w%) with 50 w/w% of ionic liquid 4-(3-butyl-1-imidazolio)-1-butanesulfonic acid triflate, to fabricate soft 3D micropillar electrodes for MEAs. These authors observed that the micropillar showed an impedance (measured at 1 kHz) of about $Z = 6*10^5$ Ω, which is more than one order of magnitude lower compared with that of the platinum planar electrodes [81].

Finally, biocompatible epoxy resins, such as the epoxy resin poly (ethylene glycol)diglycidyl ether (PEGDE) can be also used as conductive fillers and crosslinkers in PEDOT:PSS films. For instance, PEGDE was found to be optimal at a concentration of 3 w/v% in PEDOT:PSS (Sigma Aldrich) [82]. Particularly, a crosslinking mechanism was detected by an X-ray Photoelectron Spectroscopy (XPS) analysis between the PEGDE epoxy ring and the sulfonic groups of PSS chains. The interaction between PEDOT:PSS and PEDGE was further verified by FT-IR spectra, with an increase in $S = 522 \pm 48$ S/cm. Moreover, the resulting composite revealed good cell viability and hydrophilic behavior with C3H10 mouse embryonic fibroblasts. Table 2 reports a general overview of the aforementioned methods to gain or increase the conductivity of PEDOT:PSS, with biocompatible compounds.

3. Tailoring PEDOT:PSS stability and adhesion enhancement in wet conditions/saline solution

Most of the electrochemical and bioelectronic applications require the stability of PEDOT:PSS constructs in aqueous or physiological solutions, after immersion [83]. However, soaked PEDOT:PSS easily faces swelling, delamination, and redispersion, due to the presence of high hydrophilic PSS chains, mostly present on the surface of the films [29]. Indeed, this excess of PSS is expected to dissolve when immersed in water, due to the formation of hydrogens bonds by HSO_3^- groups [29]. In this way, the film becomes hydrophilic. This disadvantage is also much more evident in PEDOT:PSS films when are produced via patterning or layer-by-layer (LBL) deposition techniques [84]. Moreover, a reduction in S has also been observed in moist air conditions [85,86].

Several methods have been reported to obtain a crosslinking of PEDOT:PSS for long-term bioelectronic applications. The crosslinking mechanism is used to avoid post-process delamination or redispersion, favouring a stable solid-state PEDOT:PSS film in wet conditions by the introduction of chemical (preferably covalent) bonds. This can be achieved by multiple crosslinking techniques, such as ultra-violet (UV) light, ionic liquids, or the use of silanes, with notable attention towards the crosslinker glycidoxy propyltrimethoxysilane (GOPS) [82]. The latter, as Håkansson et al. [84] demonstrated, showed an increase in water stability already at low levels, such as 0.1 v/v% in PEDOT:PSS (Clevios™ PH1000 and Clevios™ PVPAI4083) spin-coated thin films. The authors explained that the epoxy ring group in GOPS reacts with the sulfonic groups of the PSS chains, leading to a change in PEDOT:PSS films morphology, while no effects occur on the oxidation level of PEDOT (see Fig. 4A, B). An incremental reduction in the globular grain-like structure of pristine PEDOT:PSS (RMS of ca. 2.1 nm) was also observed with an increase in the concentration of GOPS (RMS of ca. 0.8) [84]. GOPS can however dramatically reduce both electrical and ionic conductivity of PEDOT:PSS. The decrease in S is mostly caused by a reduction in charge carrier mobility, due to the insulating properties of the siloxane network. Instead, a high drop in ionic conductivity can be caused by a direct reaction of GOPS with PSS regions, where ions move. Precisely, S could drop by one order of magnitude at 0.1 v/v% of GOPS in PEDOT:PSS, with a further decrease as far as PSS units exceed GOPS molecules, and finally saturates at 1.0 v/v% of GOPS, with S = 0.002 S/cm [84]. This behavior has been also reported by Zhang et al. [21], which demonstrated that the addition of GOPS in a PEDOT:PSS:DBSA:glycerol mixture caused an increase of the film thickness and a decrease in S, despite GOPS prevented film dissolution and delamination after immersion in water (see Fig. 4C). Furthermore, ElMahmoudy et al. [88] demonstrated that a GOPS addition (ranging from 0.05 to 5.0 w/w%), in a PEDOT:PSS (Clevios™ PH1000) aqueous solution with EG (5.0 w/w%) and the surfactant DBSA (0.002 v/v%), significantly affected the bulk

Table 2
Chemical mechanisms to enhance conductivity in PEDOT:PSS by means of biocompatible compounds: typologies used for bioelectronic applications with relative additives and conductivity values.

Chemical mechanisms for biocompatible PEDOT:PSS conductivity enhancement					
Compound	Concentration	PEDOT:PSS typology	Conductivity *ante doping*	Conductivity *post doping*	Ref.
Organic solvent addition					
Dimethyl sulfoxide (DMSO)	2.0 w/w%	High conductivity grade (Sigma Aldrich) (2.2–2.6 wt%)	10^{-2} S/cm	200 S/cm	[68]
	13 v/v%	Clevios™ PH 1000 (Heraeus) (1.1 w/w %)	<10 S/cm	~20 S/cm	[15]
	17.0 w/w%	Baytron P V4071	0.07 S/cm	73 S/cm	[66]
4-Dodecylbenzenesulfonic acid (DBSA) and glycerol	Glycerol (5.0 v/v%) – DBSA (0.5 v/v%)	Clevios™ PH 1000 (Heraeus) (1.1 w/w %)	<1 S/cm	600–700 S/cm	[21]
Ethylene glycol (EG)	6.0 v/v%	Clevios™ PH 1000 (Heraeus) (1.1 w/w %)	<10 S/cm	1418 S/cm	[67]
Co-solvent system	80.0 v/v% ACN – 20.0 v/v% water	Clevios™ P(Heraeus) (1.3 w/w %)	0.2 S/cm	103 S/cm	[62]
Others	Hydrothermal treatment (HT) (relative humidity >80 %, heating temp. >61 °C)	Clevios™ P (Heraeus)	0.495 S/cm	125.367 S/cm	[55]
Surfactant treatment					
Polyethylene glycol (PEG)	Mw_{PEG} 400 (0.04 mol/L)	Bayer AG PEDOT:PSS	0.1 S/cm	17.7 S/cm	[52]
	Mw_{PEG} = 400 (4.0 v/v%)	Clevios™ PH 1000 (Heraeus) (1.1 w/w%)	few S/cm	1399 ± 87 S/cm (after methanol soaking)	[80]
Others					
Biocompatible ionic liquids (organic or inorganic salts), biocompatible epoxy resins (poly(ethylene glycol)diglycidyl ether (PEGDE)					

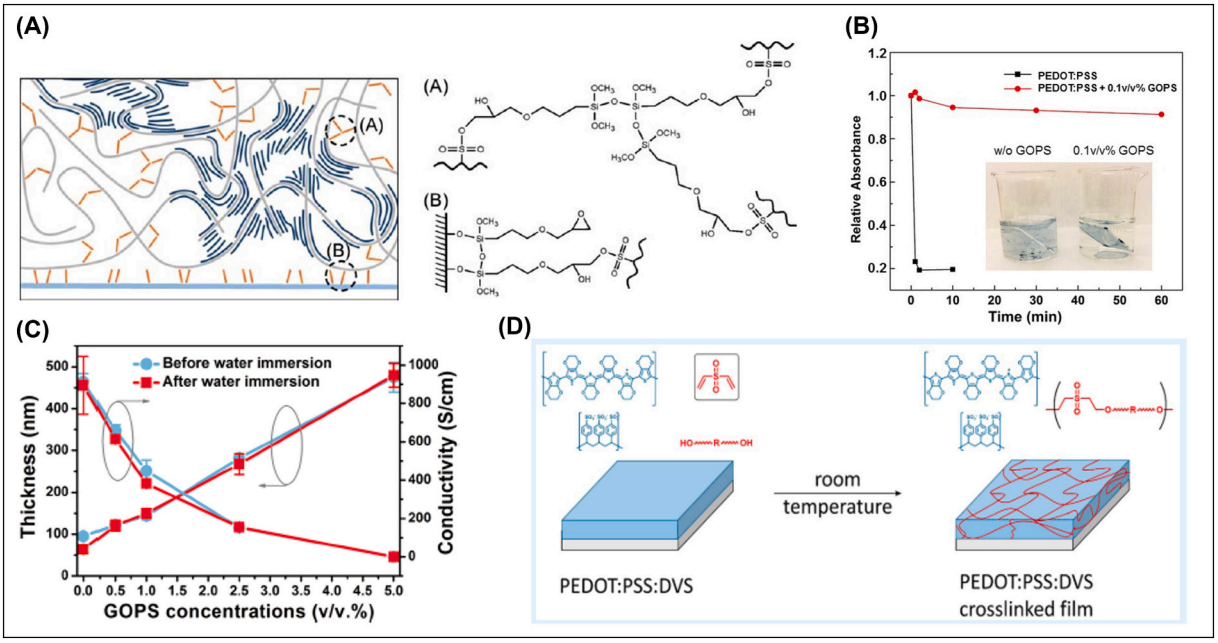

Fig. 4. Tailoring PEDOT:PSS stability in wet conditions: a selection of representative cases. (A) Schematic representation of the GOPS-crosslinked PEDOT:PSS mechanism (Clevios™ PH1000): (a) zoom on the GOPS interaction with PSS-chains, showing a chemical bonding between HSO_3^- groups of PSS and GOPS epoxy ring, and between three GOPS molecules; (b) zoom on the GOPS methoxysilane chemical bonding with glass surface hydroxyl groups. (B) Relative absorbance with respect to pristine and GOPS-crosslinked (0.1 v/v%) PEDOT:PSS films on glass substrate at different water immersion times. Republished with permission from Håkansson et al. [84], Copyright© John Wiley and Sons 2017. (C) Effect of GOPS concentration on the thickness and conductivity of PEDOT:PSS films (Clevios™ PH1000), doped with 5.0 v/v% glycerol and 0.5 v/v% DBSA. Republished with permission from Zhang et al. [21], Copyright© AIP Publishing 2015. (D) Schematic illustration of the DVS cross-linking reaction in PEDOT:PSS films (Clevios™ PH1000) at room temperature. Republished with permission from Mantione et al. [87], Copyright© American Chemical Society 2017.

conductivity in the film; the highest *S* (~460 S/cm) was observed for the film containing a GOPS amount of at least 0.05 w/w%, whereas *S* decreased by four times (120 S/cm) with a GOPS concentration of 5.0 w/w%. Contrary, the ability of the PEDOT:PSS film to uptake water (swelling capacity) decreased, especially from 397 % to 12 % when the GOPS content increased from 0.05 to 5.0 w/w%. Therefore, although GOPS uptakes loss in conductivity, its convenience with respect to water stability enhancement induced several researches to still investigate its content effect at low concentrations. Dijk et al. [89] used an aqueous dispersion of PEDOT:PSS (Clevios™ PH1000) in a mixture of EG, DBSA,

and GOPS as a coating material for MEAs (64 gold electrodes with a diameter of 20 μm). After four months of incubation in cell culture media, >70 % of the electrodes did not show visible signs of degradation (stable average $Z = 25.5 \pm 3.4$ kΩ at 1 kHz at day 112), validating the use of GOPS. Guex et al. [90] also obtained a stable $S = 6.1 \pm 4.0{*}10^{-6}$ S/cm after 28 days in cell culture media, by mixing a PEDOT:PSS aqueous dispersion (1.25 w/w%, Ossila Ltd., Sheffield, UK), with 0.25 v/w% DBSA, and 0.0, 1.0, 2.0 or 3.0 v/w% GOPS.

Another disadvantage of GOPS is the necessity to use high curing temperatures (conventionally 140 °C for 1 h), which does not allow the biofunctionalization of the compound with natural biomolecules, due to their high potential degradation. Alternatives to GOPS have been then investigated in the recent years. Mantione et al. [87] used dispersions of PEDOT:PSS (Clevios™ PH1000) in a mixture of EG (5.0 v/v%, DBSA (0.1 v/v%) and divinylsulfone (DVS) as crosslinker agent for the preparation of films used in OECTs bioelectronic applications (see Fig. 4D). DVS is a reactive molecule, which has been widely studied to crosslink biomolecules such as glycosaminoglycanes (GAGs) and hyaluronic acid. Its main features include: a high reactivity with nucleophiles such as alcohols, thiols and amines, the possibility to work in a wet environment, and a low b.p. which facilitates the elimination of PSS excess [87]. The PEDOT:PSS films crosslinked with DVS presented $S = 550–750$ S/cm, that is 200–300 S/cm higher than that of the PEDOT:PSS films crosslinked with GOPS at 3.0 v/v%, indicating that the addition of DVS did not drastically affect the conductivity [87]. Moreover, a better transconductance of 13.2 ± 0.65 mS (day 10), and stability of thin PEDOT:PSS-DVS films were achieved in a sterile phosphate buffered saline (PBS) solution, when compared to PEDOT:PSS-GOPS samples [87].

Alternatively to DVS, the addition of biomacromolecules to PEDOT:PSS, such as proteins, enzymes, or electrocalysts, like metal or metal oxide nanoparticles and carbon-based nanomaterials [20], has been also explored for increasing PEDOT:PSS stability in water. Zhang et al. [20] investigated the use of sodium carboxymethyl cellulose (NaCMC, 1 mg/mL in double-distilled water) as stabilizer in PEDOT:PSS (Baytron P, 1.3 w/w%) films on glassy carbon electrodes (GCEs). NaCMC is a water-soluble, non-toxic, anionic biopolymer, usually implemented as food additive or binder for the production of Si anode in Li-ion batteries [91–93], due to its good ionic conductivity which facilitates the movement of Li^+ ions. Those films revealed a good adhesion and electrocatalytic ability as electrochemical sensors for individual or simultaneous detection of different agricultural harmful substances and nutritional ingredients, such as salicylic acid, nitrite, and maleic hydrazide. Indeed, PEDOT:PSS-CMC/GCE film retained ca. 99.4 % of its original activity for 105 days, using $[Fe(CN)_6]^{3-/4-}$ as redox couple and 0.1 M of potassium chloride (KCl) as electrolyte. Its electrical stability was further confirmed by cyclic voltammetry (CV) tests for 300 cycles, resulting in an integral area decrease of only 6.7 %. Moreover, PEDOT:PSS-CMC films showed robust structural flexibility after soaking in water for ca. 35 days, with almost no change in the surface morphology. The PEDOT:PSS-CMC conductivity (S ca. 1.05 S/cm) also gradually increased after immersion in double-distilled water till $S = 20.4$ S/cm at day 10, due to a surface loss of excess PSS chains in the film conformation, despite at longer soak times, a decrease was detected due to film damage ($S = 8.5$ S/cm at day 40) [20]. This drop in conductivity may be caused by unorganized interconnected PEDOT-rich regions, despite the segregation of PSS and CMC [16]. Belaineh et al. [16] blended PEDOT:PSS (Clevios™ PH1000, 1.1 w/w%) with CMC and cellulose nanofibrils (CNF) separately, for the fabrication of continuous nano-beadlike structures with π-stacked PEDOT or structures dominated by phase separation with lamellar stacking of PEDOT, respectively. AFM and TEM observations showed that CNF-PEDOT:PSS had a more organized structure than CMC-PEDOT:PSS, especially in the presence of a secondary dopant (DMSO), favouring mechanical stability and a higher conductivity.

Another alternative crosslinker to GOPS is poly(ethylene glycol) diglycidyl ether (PEGDE), that is a water soluble epoxy resin. Solazzo et al. [82] fabricated homogenous films with PEDOT:PSS (Sigma Aldrich) and PEGDE at concentrations of 0.0, 1.0, 3.0, 5.0, 10.0 w/w%. After a post-curing process at ambient temperature, PEDOT:PSS-PEDGE 3.0 w/w% reached an interesting value of $S = 706 \pm 32$ S/cm, exhibiting a similar stability to PEDOT:PSS-GOPS films at 3.0 v/v% (after 48 h in distilled water, room temperature). Relevant results have been also obtained with the use of the biocompatible photoactive crosslinker poly (ethylene glycol) diacrylate (PEGDA), commonly applied in biomimetic interfaces. Particularly, Polino et al. [48] produced PEDOT:PSS (Clevios™ PH1000) - PEGDA (8.0 w/w%) films, with EG at 6.0 w/w%, by spin and spray coating techniques, and further functionalized with poly-L-lysine (PLL) at 0.01 v/v% (aqueous solution). PEGDA was shown to influence the PEDOT:PSS surface roughness, increasing it till 300–580 nm at 17.0 w/w% (spray coating), while generating defects at low concentrations (2.0 w/w%), due to a poor solubility. The thin films biocompatibility was still verified with primary fibroblasts.

A long-term, stable adhesion of PEDOT:PSS films to the substrate is also necessary to prevent easy peel-off or crack formation. Surface treatments, such as UV, plasma cleaning (e.g. air, nitrogen, oxygen) or chemical ones can be applied. For instance, hydroxyl groups are usually generated on PDMS substrates to reduce its high hydrophobic behavior [94]. Alternatively, GOPS and DBSA crosslinkers can avoid delamination and detachment on different type of substrates, such as glass. When using plastic substrates, like polyethylene terephthalate (PET), such crosslinkers can be also avoided; Zhang et al. [95] indeed demonstrated that PEDOT:PSS (Clevios™ PH1000) spin coated films on PET, with glycerol as secondary dopant, remained intact in wet conditions also after 90 days.

In the case of flexible and wearable bioelectronics, glycerol, polymeric blends (as poly(vinyl alcohol), PVA and PEG), or ionic liquids can be also useful to increase PEDOT:PSS stretchability, by reducing the ionic interaction between PEDOT and PSS chains [96,97]. Wang et al. [22], studied the incorporation of PVA (10 % v/v) into a drop-casted PEDOT:PSS (1.3 w/w%, Bayer AG) dispersion on GCE substrates. This composite revealed excellent film forming and adhesive properties, useful in electrochemical sensors. PVA (2.0 w/w%) was also investigated by Lu et al. [98], in combination with poly(acrylic acid) (PAA), for the generation of an interpenetrating network (IPNs) with PEDOT:PSS (Sigma Aldrich) to enhance its adhesion of platinum electrodes arrays for in-vivo opto-neural tissue interfaces. The resulting polymer-hydrogel showed reduced electrochemical impedance and higher capacitance at 1 kHz.

4. PEDOT:PSS biocompatibility assurance and enhancement

Biocompatibility, surface topography, mechanical, conductive, and chemical properties are necessary to obtain a functional bioelectrical interface. Since their discovery, CPs have been applied as electroactive substrates for the growth and modulation of electrically active cells. Due to their ionic-electronic nature, they have been used as electroactive materials for TE interfaces in the form of electrodes (alternative to metal-based ones), hydrogels (see Fig. 5A), or surface coatings. Their permeability to ions can enlarge the electrochemical surface area of the electrode, while keeping its geometric surface area, with no loss in sensitivity (high signal-to-noise ratio) or charge injection [96,99].

Pristine PEDOT:PSS has been widely evaluated biocompatible for both in-vitro (cytotoxicity assays and cell culturing) and chronically in-vivo studies [100]. Specifically, it has been mostly exploited in novel soft and stretchable electrodes for its high charge storage capacity and its relatively low interfacial impedance, which allows its use for long-term periods. Moreover, another significant benefit of utilizing PEDOT:PSS is its optical transparency when fabricated as thin film, offering the potential for simultaneous optical and electronic transduction within a single experiment, making it useful for many electronic and optoelectronic devices [79,101,102]. By controlling the film thickness

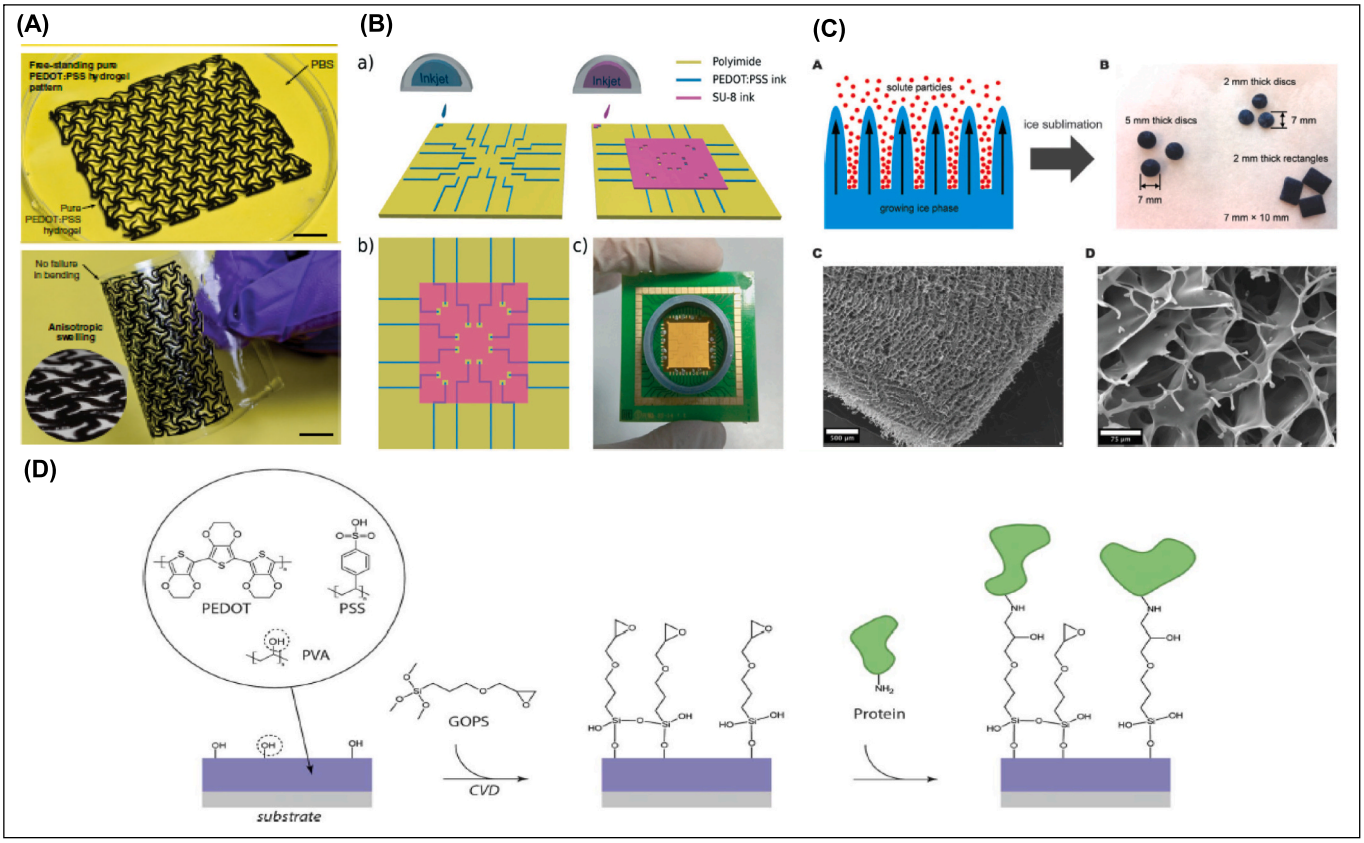

Fig. 5. Representative applications of biocompatible PEDOT:PSS constructs. (A) Pure PEDOT:PSS hydrogels (Clevios™ PH1000) on PET substrate showing an anisotropic drying process. Republished with permission from Lu et al. [15], Copyright© Springer Nature 2019. (B) A PEDOT:PSS ink-jet printed MEA (Clevios™ PJet 700, with 10.0 w/w% glycerol) validated with cardiac cells for in-vitro electrophysiological recording: (a) production strategy and materials adopted, (b) MEA design composed of 16 electrodes, and c) integrated MEA in a standard MEA PCB 64-electrode chip layout. Republished with permission from Garma et al. [76], Copyright© Royal Society of Chemistry 2019. (C) PEDOT:PSS (Clevios™ PH1000) scaffolds made with an (a) ice templating technique (b) of various shapes, such as disks and rectangles; SEM images of (c) PEDOT:PSS scaffolds with the addition of 3.0 w/w% GOPS, (d) with zoom on the porous structure. Republished with permission from Wan et al. [106], Copyright© Royal Society of Chemistry 2015. (D) Representative scheme for the functionalization of PEDOT:PSS by PVA incorporation (Clevios™ PH1000). Republished with permission from Strakosas et al. [107], Copyright© Royal Society of Chemistry 2014.

(usually in nano scale) and the blend composition [103], PEDOT:PSS can indeed serve as a transparent electrode in the visible range [104] with a transparency up to 90% [105], which is very useful in applications where visibility is essential, such as in cellular monitoring over time, organic solar cells, or organic light-emitting diodes (OLEDs). Particularly, systems which uses PEDOT:PSS transparent electrodes in cellular monitoring are able to perform direct cell imaging using conventional inverted optical microscopy, all while maintaining effective recording of electronic signals, such as cellular impedance [108,109]. However, its biocompatibility must be ensured even after the addition of (co-)solvents, ionic liquids, and/or crosslinkers. As explained by Berggren et al. [99], due to the synthesis method and the manufacturing process chosen, the PEDOT:PSS film might potentially retain residues like monomers, solvents, additives or an excess of dope-ions. If these elements, referred as cytotoxic residuals, are released from the film over the course of an experiment in the medium culture, they can provoke a high risk of toxicity, leading to cellular damage or even death [99]. Long detoxification processes are then required to remove these cytotoxic compounds (if feasible) [110]. In the next paragraph, representative studies on the use of PEDOT:PSS as coating material, thin film/electrode, and scaffold are presented, with special attention to biocompatibility and the effect on cellular lineages.

One of the main applications of PEDOT:PSS in bioelectronics is as coating material on conductive electrodes for in-vitro electrophysiological recording [111,112] or as wearable OECTs for non-invasive detection of bioanalytes and/or signaling molecules, such as glucose [113] and dopamine. Blau et al. [114] studied for 63 days the activities of cortical and hippocampal brain tissue cells of embryonic rats cultured on fully polymer MEAs, composed of PDMS coated with PEDOT:PSS (CPP105D, H.C. Starck, 1.2 w/w%) and EG (5.0 v/v%). Results showed a good cellular network morphology, with a survival rate similar to the one obtained on commercial non-polymer MEAs (control sample). Similarly, Garma et al. [76] cultured cardiomyocyte-like cells on MEAs printed with a mixture of PEDOT:PSS (Clevios™ PJet 700) and glycerol (10.0 w/w%) (See Fig. 5B). An average of 94.90 % of living cells was reached after 48 h, showing a good biocompatibility of the device. Hempel et al. [115] also reported the successful use of PEDOT:PSS-based (Sigma Aldrich) OETCs for electrophysiological sensing of cardiac cell line HL-1. 3D MEAs devices, equipped with PEDOT:PSS-based (Clevios™ PH1000) micropillar electrodes, doped with the ionic liquid 4-(3-butyl-1-imidazolio)-1-butanesulfonic acid triflate (IL, 50.0 w/w%), were also effectively used for the culturing of mouse cardiac muscle cells, revealing how the local mechanical microenvironment generated by the micropillar electrodes was highly compatible with that of in-vivo tissue [81].

Regarding in-vivo studies, Zheng et al. [116] reported the 3D printing of PEDOT:PSS (3 w/w%, Clevios™ PH1000) using a room-temperature DBSA 10.0 w/w% coagulation bath, for the fabrication of a cortex-wide neural interface for mice brain activity stimulation. Results showed a high charge injection capacity (CIC), $CIC = 6.366$ mC/cm^2 and a maximum Z of 14.9 $\pm$ 0.54 kΩ at 1 kHz in vivo after three-weeks post-implantation.

PEDOT:PSS has been also utilized as stand-alone electrode for electrophysiological analyses. Pires et al. [117] modulated the neurite outgrowth of human neural stem cells (NSC) through electrical stimulation, resulting in 1.6 times higher than the one in non-stimulated conditions. The electrodes were composed of a mixture of PEDOT:PSS (Clevios™ P AI 4083, solid content 1.3–1.7 %), EG (volume ratio 1:4), DBSA (0.5 μL/mL), and GOPS (10 mg/mL). Alternatively, Ganji et al. [118] investigated the use of PEDOT:PSS (Clevios™ PH1000) in a mixture with EG (~20.0 v/v%), DBSA (0.2 v/v%), and GOPS (1.0 w/w %) as electrodes on Parylene-C flexible substrate for an in-vivo intra-operative monitoring of human brain. The 56 microelectrodes (Ø ~ 50 μm) in the device showed a functionality of ca. 96 %, and displayed impendences 10 times lower than platinum electrodes (ca. 12.63 kΩ vs 314.79 kΩ, respectively) in the frequency range for physiological analyses of [1 Hz–10 kHz]. Through the device, the evoked cognitive activity was shown, with changes in amplitude of ca. 400 μm. Won et al. [110] also developed water-stable PEDOT:PSS (1.1 w/w%) hydrogels via phase separation induced by a laser source, with a final $S = 670$ S/cm and a resolution down to 6 μm in water. The hydrogels were blended with plasmonic AuNPs (0.1 w/w%, Ø = [40–60] nm) and they showed a $CIC = 16.17$ mC cm^{-2}, long stability after 10,000 cycles of pulses and 6 months, and good neural signal recording from a brain slice of mice.

TE applications often use PEDOT:PSS for the fabrication of thin films or scaffold-like constructs to support in-vitro cellular activity too. For instance, Han et al. [119] developed a flexible PEDOT:PSS-based hydrogel optoelectronic interface, for the generation of action potentials in neurons and cardiac myocytes below 50 and 150 mW cm^{-2}, respectively. The interface owns a Young's modulus in the range of 33–40 kPa, a stable charge injection of 13.2 ± 1.4 μC cm^{-2} under 50 mW cm^{-2} (in the presence of DMSO at 16.0 v/v%), and a long-term functional stability, demonstrated by accelerated aging tests at 87 °C, in which the photovoltage retained by 92 ± 2.8 % after 4.5 weeks of testing, which is equal to ~36 months. Marzocchi et al. [29] instead studied the effect of surface roughness, surface conductivity, wettability, and surface energy on spin coated PEDOT:PSS films (Clevios™ PH1000 and CPP105D) for a controlled cellular growth of glioblastoma multiforme cells (T98G) and primary human dermal fibroblasts (hDF). Electrochemical polymerization of the PEDOT:PSS films was performed by means of an external redox voltage at different oxidation states (redox voltage of −0.9 V and +0.8 V), and in different aqueous media, such as PBS. Cells were seeded on reduced, oxidized, and not biased samples and after 72 h, a strong cell-dependency effect was only present on the electrochemical state of the film; the proliferation rate of T98G cells was highly enhanced on reduced samples, while for hDF only on the oxidized PH1000, showing in both cases a strong chemical interaction with the culture media. Also Wan et al. [106] discovered that oxidized 3D microporous PEDOT:PSS (Clevios™ PH-1000) scaffolds promoted the adhesion and growth of mouse fibroblasts (3T3-L1) (7 days) better than reduced ones by 1.5 fold (see Fig. 5C). Particularly, scaffolds were produced via an ice-templating method and doped with GOPS (3.0 w/w %). Scaffolds also showed a good electrochemical switching behavior. Alternatively, Amorini et al. [120] demonstrated that the redox state of PEDOT:PSS (Clevios™TM CPP105D) films can be electrically modulated to obtain a sponge effect on ions at the film-liquid interface, allowing a change in the ionic environment around cells, thus the ability to govern cellular adhesion, viability, and growth. 3D anisotropic porous PEDOT:PSS (Sigma-Aldrich) scaffolds have been also obtained by Solazzo et al. [47] and tested on C3H10 mouse embryonic fibroblasts. Specifically, a lyophilization (freeze-drying) process, followed by crosslinking with GOPS, and subsequent exposition to a sulfuric acid crystallization for PSS removal and PEDOT nanofibrils generation, was performed. The same authors also demonstrated a discrete cell viability (above 85 %) of mouse embryonic fibroblasts on PEDOT:PSS crosslinked with 1.0 and 3.0 w/w% of PEGDE, and on PEDOT:PSS crosslinked with 3.0 w/w% of GOPS [82]. Murine fibroblast cells cultured on PEDOT:PSS-GOPS and PEDOT:PSS-DVS films (Clevios™ PH-1000), showed instead a viability comparable to the inert control (polyethylene) already at 24 h [87]. PEDOT:PSS crosslinked with DVS (3.0 v/v%) also evidenced a better initial cellular adhesion for human neuroblastoma cells, when compared to PEDOT:PSS crosslinked with GOPS, being beneficial for the establishment of a neural interface. Alternatively, Guex et al. [90] proposed highly porous freeze dried PEDOT:PSS (1.25 w/w% in aqueous solution, Ossila Ltd) scaffolds doped with DBSA (0.25 v/v%) and GOPS (0.0, 1.0, 2.0 or 3.0 v/v%) as secondary dopant and crosslinker, respectively. The resulting scaffolds were further cultured with MC3T3-E1 osteogenic precursor cells, demonstrating the ability to increase ECM mineralisation and osteocalcin deposition. A precursor cellular differentiation into osteocalcin positively stained osteoblasts after 28 days, and enhanced levels of genes, such as alkaline phosphatase, runt-related transcription factor 2, and collagen type I alpha 1 were observed, along with a deposited mineralized extracellular matrix (ECM).

PEDOT:PSS can be also biofunctionalized in its bulk or surface with biomolecules or side-groups of the ECM, in order to improve the biological interface and encouraging cellular viability [99]. Especially, this biofunctionalization is usually performed after fabrication to avoid any potential denaturation of the biomolecules, due to an exposition to solvents and high annealing temperatures. For instance, Strakosas et al. [107] proposed a method to easily incorporate biomolecules after film preparation, as shown in Fig. 5D. Before film casting, PVA (Mw_{PVA} = 130,000) was added into a mixture of PEDOT:PSS (Clevios™ PH 1000), DBSA (0.5 mL/mL), and EG (50 mL/mL); later a silane reagent was chemically vapor deposited onto the film, and glucose oxidase (GOx) and ECM-derived polypeptide poly-Llysine (PLL) were finally incorporated in the film. Silane reagents (e.g. aminosilanes, APTS (3-aminopropyltriethoxysilane) or GOPS usually contain an organic functional group which can bind a secondary organic molecule and an alkoxylane. Thus, they can produce a covalent linkage with the free hydroxyl groups of the substrate surface (usually glass or metal oxide based), via a condensation reaction.

5. Remarks regarding PEDOT:PSS and biodegradability

CPs, including PEDOT:PSS, are not officially classified as biodegradable materials. However, in the past decade, efforts have been made to develop biodegradable composites within this category. As stated by Peng et al. [121], biodegradation is a phenomenon caused by enzymes or chemical degradation actuated by living organisms and/or their secretions. In the context of TE, biodegradability refers to a material capability to degrade at a certain rate which aligns with the natural growth or regeneration of native tissues over time, thus eliminating the need for surgical removal [7]. Biodegraded organic polymers undergo breakdown into smaller molecules, eventually transforming into carbon dioxide and water, usually through hydrolysis and oxidation [122]. As explained by Boehler et al. [123], to ensure material biodegradability, there are primarily two approaches: creating a composite with a biodegradable substance or altering the material backbone structure. This alteration involves introducing enzymatically cleavable or hydrolyzable linkages between smaller electronic segments. This approach is designed to ensure that even small portions of non-degradable segments can potentially be tolerated and eliminated or phagocytized without causing tissue irritation or inflammation.

In the wide context of CPs, this corresponds to finding a balance between conductivity and biodegradability. Until recently, there have been relatively few studies exploring PEDOT:PSS composites with potential biodegradability. For example, Ren and Dong [124] introduced an electrohydrodynamic electrode composed of PEDOT:PSS (PEDOTinks)/Graphene/PVA for foldable electronics, which, after a 10-day exposure to a water-based plant microbial solution, displayed a significantly rougher surface compared to the one obtained when immersed in DI water. This surface modification suggests a potential degradation, as it appeared to serve as a nutrient source for microbials. Zhuang et al. [125] also investigated a potential biodegradable film made of Silk

Fibroin/PEDOT:PSS (Clevios PH™ 1000) designed for electroactive cell culturing, as evidenced by their experiments with PC12 cells. In their study, the film was immersed in a solution containing 0.1 U/mL protease XIV, an enzyme typically utilized for investigating silk degradation. After a span of 4 weeks, the film exhibited a weight loss of >20 %, and, despite the poor degradability of PEDOT:PSS, the conductive layers located on the surface of the film surface showed a minimal presence of PEDOT:PSS.

Despite these achievements, it is important to note that no in-vivo investigation was conducted to assess biodegradability. Indeed, there is still a considerable gap from achieving a truly biodegradable PEDOT:PSS suitable for use in the field of bioelectronics.

6. Tailoring PEDOT:PSS bioelectrical properties with carbon fillers

Recently, carbon-based materials, such as graphene, graphene oxide (GO), reduced graphene oxide (rGO), carbo nanotubes (CNTs), graphite, carbon black, and carbon materials derived from natural-biomaterials, have attracted wide attention due to their unique chemical-physical properties. Such properties refer to a good electrical conductivity, a high chemical and thermal stability, and in general a low toxicity [126]. Especially, as reported in Fig. 6A, different forms of nanocarbons such as graphene and its derivatives (i.e. planar graphene, porous graphene and out-of-plane grown 3D graphene flakes), and nanocrystalline diamonds have found application in bioelectronics [127]. In particular, nanosized conductive fillers have been explored for the development of polymer-based conductive composites [128], thus the electrical conductivity of PEDOT:PSS can be further enhanced by their incorporation. CNTs and graphene matrices are usually incorporated in PEDOT:PSS structures for optoelectronics and organic OECT [129]. It is known that the carbon-based fillers form conductive paths within the polymeric matrix, improving its conductivity [130]. However, the formation of such conductive paths is affected by the distribution, amount, shape, and intrinsic properties of the fillers. Therefore, the choice of the preparation method and compound concentrations are important to obtain the desired level of filler dispersion. At a certain critical loading value, known as percolation threshold, S starts to increase of many orders of magnitude with a very small increase in the filler loading [128]. The percolation threshold value also decreases with an increasing aspect ratio (ratio between length and diameter) of the filler [131].

Next paragraphs present the most interesting carbon fillers implemented in bioelectronics, along with a portfolio of selected cases which highlight their incorporation in PEDOT:PSS and benefits. Table 3 eventually summarizes those findings.

6.1. Graphene, derivatives, and their incorporation in PEDOT:PSS

Graphene is a single layer of sp^2 hybridized carbon atoms and typically has a honeycomb structure [134]. Graphene and its derivatives, i.e. 2D planar graphene, 3D porous graphene, out-of-plane/vertical graphene, GO, and rGO, have been explored for bioelectronics due to their high electrical conductivity (10^4–10^5 S/m) [135], mechanical strength, flexibility, transparency, surface area (2630 m^2/g for monolayer graphene) [136], chemical stability, and tunability [127]. In addition, graphene can be easily dispersed in aqueous-based solutions for the formulation of conductive mixtures [10]. Planar graphene can be produced by several methods and the current price for graphene powder ranges between $ 50–$ 200/kg, depending on quality and volume of purchase [137]. A low cost and large-scale method for the production of planar graphene is the chemical exfoliation based on the preparation of a GO suspension starting from graphite using the Brodie, Staudenmaier or Hummers method, followed by the reduction of GO using thermal, UV or chemical treatments [138]. Alternative methods to synthesize graphene are the epitaxial growth on silicon carbide (SiC), which involves a thermal decomposition of SiC at 1200–1700 °C under high vacuum [139], and the chemical vapor deposition (CVD) based on the thermal decomposition of carbon precursor gases on metals catalysts, such as Ni, Co, and Cu-based substrates, at high temperatures (~1000 °C), under ambient pressure or low pressure conditions [140]. The method used to synthesize planar graphene can affect its chemical and physical properties, such as size distribution, surface chemistry (i.e. surface functional groups and surface charge) purity, and, as a consequence, the interactions of graphene with cells and tissues [141]. For example, monolayer graphene substrates synthesized by CVD at low pressure, have been reported to promote both proliferation of fibroblasts and differentiation of neurons [142]. However, pristine graphene has been also described to be toxic for renal cells, macrophages, and red blood cells due to a high level of oxidative stress [143,144]. Therefore, the cytotoxicity of graphene can be reduced through surface functionalization [145]. As documented by Guo et al. [146], the primary methods include covalent, non-covalent, nanoparticle functionalization, and plasma hydrogenation. Covalent functionalization involves the formation of covalent bonds and can be accomplished using substances like DNA, polymers, or proteins. Conversely, non-covalent functionalization can be achieved through polymeric grafting or interactions like π–π bonding with small molecules containing aromatic rings or surfactants. Binding nanoparticles (NPs) to the surface, achieved by reducing metallic salts with agents like sodium citrate or ethylene glycol, is also a well-established option. Lastly, hydrogenation of graphene using argon or hydrogen plasma is a relatively new, straightforward approach, which can reduce contamination during the process and enhances hydrophilicity. Alternative approaches, like PEGylation, are applicable for in-vivo studies. In such scenarios, PEGylation serves to minimize the formation of a protein corona when nano-sized graphene interacts with blood components.

Among graphene-based materials, porous graphene has been synthesized by various methods: (i) self-assembly of GO nanosheets [147], (ii) template method (including template-directed assembly and template-directed CVD) [148], and (iii) laser scribing method starting from commercial polymers [149]. Notably, porous graphene, synthesized by template-directed CVD method, has been reported to have high biocompatibility and enhance the differentiation of neural stem cells towards astrocytes and neurons [150]. Out-of-plane graphene flakes have been instead produced by thermal decomposition of SiC [151] or plasma-enhanced CVD [152]. 3D fuzzy graphene has been also synthesized on a 3D Si nanowire mesh template, showing high electrical conductivity (2355 ± 785 S/m) and surface area (1017 ± 127 m^2/g) [153]. In addition, scaffolds based on out-of-plane graphene flakes have been reported to own high biocompatibility and promote the proliferation of osteoblasts [154]. As stated by Uz et al., this cellular-graphene interaction is most probably caused by π–π interactions of aromatic amino acids found in the cellular membrane which orient proteins towards the graphene layers [10].

The incorporation of graphene in PEDOT:PSS has been extensively exploited in electrophysiological interfaces (MEAs devices), biosensors, bio-actuators, and drug delivery carriers. For instance, Kshirsagar et al. [155] fabricated MEAs based on PEDOT:PSS and graphene with Au conductive paths leading to the microelectrodes and negative epoxy photoresist SU-8 as insulator. Graphene was deposited on the substrate using a polymer-based transfer method, whereby PEDOT:PSS was electrodeposited on the graphene microelectrodes. The pristine graphene microelectrodes exhibited an electrochemical impedance of 21.0 Ω cm^2 at 1 kHz with a transmittance of 99.4 %. After electrodeposition of PEDOT:PSS, the impedance decreased to 0.3 Ω cm^2 at 1 kHz and the transmittance reduced to 50 %. Furthermore, the PEDOT:PSS-graphene microelectrodes recorded cardiac field potentials with amplitudes up to 3.8 mV peak-to-peak and noise below 20 μV peak-to-peak, similar to those recorded from TiN and carbon electrodes. Similarly, Lee et al. [24] deposited PEDOT:PSS-GO and PEDOT:PSS-rGO composite films on gold microelectrodes, demonstrating that both composites improved the electrochemical durability and charge storage capacity of PEDOT:PSS.

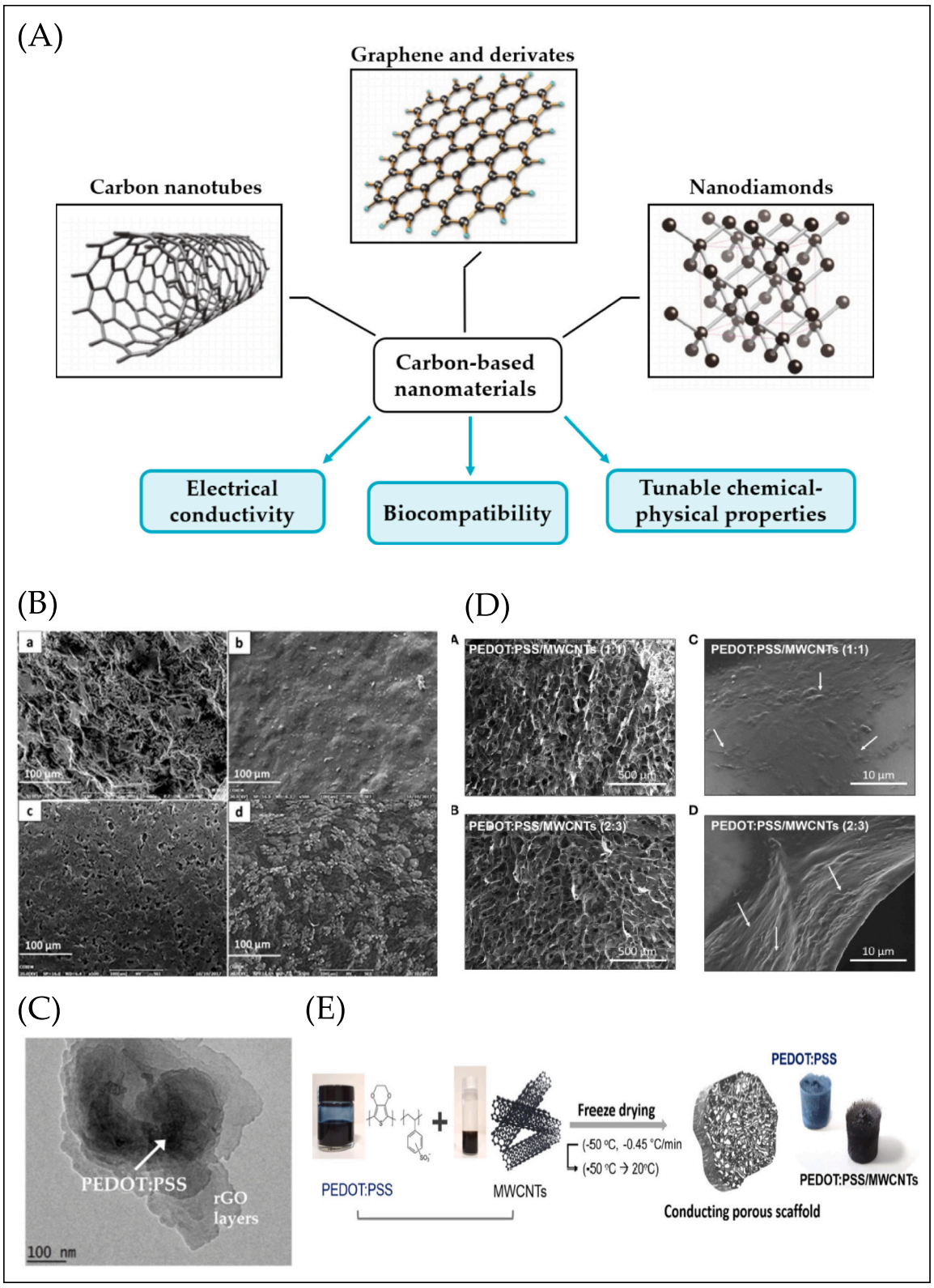

Fig. 6. Tailoring PEDOT:PSS properties with carbon fillers: (A) Carbon-based materials and their main features in bioelectronic applications; (B) SEM images of solid-state (a) rGO, (b) PEDOT:PSS, (c) GO-PEDOT:PSS, and (d) rGO-PEDOT:PSS layers deposited on a commercial screen-printed carbon electrode (SPCE), showing surface differences caused by the presence of dispersed colloidal aggregates in the interlayers spacing; (C) relative TEM image of the rGO-PEDOT:PSS composite, indicating the presence of PEDOT:PSS between rGO layers. Republished with permission from Abd-Wahab et al. [132], Creative Common CC BY license 2019. (D) SEM images of a soft-porous, solid-state PEDOT:PSS/MWCNT-based 3D scaffold at the ratios (a) 1:1 and (b) 2:3, (c, d) with highlighted (white arrow) the CNTs domains, respectively; (E) Schematic view of the process for the fabrication of 3D hybrid PEDOT:PSS and PEDOT:PSS/MWCNT conductive scaffolds. Republished with permission from Jayaram et al. [133], Creative Common CC BY license 2019.

Table 3
PEDOT:PSS for bioelectronic applications, with special focus on carbon fillers incorporation.

#	Material typology	Application	Technology	Features	Cellular lineage	Main results	Ref.
Cellular interfaces							
2	PEDOT:PSS, **SWCNTs**	MEAs	Electrodeposition	CSC (1.21 ± 0.02 mC/cm^2), *S* (323 ± 75 S/m)	Primary chicken embryonic cardiomyocytes	Excellent biocompatibility	[166]
3	PEDOT:PSS, **MWCNTs**, glycerol, EG, GOPS, CMC	MEAs	Aerosol jet printing	*C* (242 ± 70 nF at 5 mV/s), Z (128 ± 22 kΩ at 1 kHz)	Cardiomyocyte-like HL-1 cells	Cytocompatibility	[167]
5	PEDOT: PSS, **MWCNTs**, DBSA, GOPS	3D electrode for bio-interfacing and tissue engineering applications	Freeze drying	*R* ~ 7 times lower compared to neat PEDOT:PSS	TIFs	Nanostructured porous morphology, excellent cytocompatibility	[133]
7	PEDOT:PSS, **MWCNTs**, alginate	Neural interfaces	Electrodeposition	*Z* (294 kΩ at 1 kHz), *C* (4.0 F)	Human neuroblastoma SH-SY5Y cells	Good biocompatibility	[176]
8	PEDOT:PSS, **MWCNTs**, GYIGSR, RGD	Neural interfaces	Electrodeposition	*Z* (15 kΩ at 1 kHz), *CSC* (7.5032 mC/cm^2)	PC12 neural cells	Good biocompatibility	[173]
9	PEDOT:PSS, **MWCNTs**, PGSU	Strain sensor	Casting	*CSC* (1508.22 ± 3.92 μC/cm^2 for 5 wt% of CNTs)	VM cells	Elastic modulus (36.63 MPa), low cytotoxicity	[177]
10	PEDOT:PSS, **MWCNTs**, PEO, GOPS	Hemodialysis devices	Electrospinning	*S* (~1 S/cm with 3 wt% of MWCNTs)	THP1 cells	Long-term water resistance, high adhesion strength on the substrate, biocompatible	[178]
11	PEDOT:PSS, **graphene**, Au, SU8	Electrodes for recording cell signals	Polymer-based transfer method, electrodeposition	*Z* (0.3 Ω cm^2)	Chicken cardiomyocytes, transgenic mouse retina ganglion cells	Transmittance (49.7 %), recorded field potentials with amplitudes up to 3.8 mV peak-to-peak	[155]
12	PEDOT:PSS, **rGO**	Implantable electrode, biosensors, drug delivery carriers and neural interfaces	Electrodeposition	CSC (155.36 ± 14.83 mC/cm^2)	PC12 neural cells	Cytocompatibility	[24]
Biosensors							
13	PEDOT:PSS, **rGO**, Au NPs	Electrodes for detection of H_2O_2	Drop casting	Improved *S* and charge transfer resistance	/	High sensitivity and low detection limit towards H_2O_2	[156]
14	PEDOT:PSS, EG, **rGO**	Sensor for CEA	Dip coating	S (3.12 × 10^{-2} S/cm), R_{ct} (2.8 kΩ), K_{ct} ((1.9 × 10–5 cm/s)	/	Enhanced sensitivity for CEA	[157]
15	PEDOT:PSS, **GNPs**	Electrodes for detection of DA	Electro-spraying	S (105 S/cm), charge transfer resistance (54.8 Ω)	/	High stability in water, enhanced catalytic activity and sensitivity of DA oxidation	[158]

The impedance of PEDOT:PSS-rGO composites at 1 kHz decreased by about 30 % when compared to the bare gold electrode, while the charge storage capacity (CSC), $CSC = 155.36 \pm 14.83$ mC/cm^2, improved as well as the electrochemical durability in comparison to pristine PEDOT:PSS. In addition, due to the porous structure of the composites, an increase in the electrical charge conduction, the degree of oxidation and redox states of GOs, and the degree of recovered conjugated carbons in rGOs, were detected. PEDOT:PSS/rGO films cytocompatibility was verified with pheochromocytoma-derived cell line (PC12) neural cells, proving their ability to modulate the expression of specific proteins, GAP-43 and synapsin, which are involved in the axonal regeneration and intercellular communication, respectively.

Graphene-PEDOT:PSS composites have been also proposed in many types of electrochemical biosensors for healthcare and analytical chemistry due to their high electrical conductivity which allows an efficient charge transfer, necessary for the detection of analytes in electrochemical reactions. Mercante et al. [156] deposited by drop casting PEDOT:PSS, rGO, and Au nanoparticles (AuNPs) on gold electrodes for the detection of H_2O_2, associated with many pathological conditions such as diabetes, atherosclerosis and aging. Afterwards, peroxidase type II from horseradish (HRP) was immobilized on the surface of PEDOT:PSS-rGO-AuNPs-modified electrodes. The final electrode exhibited higher electrochemical activity compared to rGO and PEDOT:PSS-rGO-modified electrodes, due to its improved electrical conductivity and high surface area. Furthermore, it showed enhanced catalytic activity towards H_2O_2 with high sensitivity and low detection limit. Likewise, Kumar et al. [157] fabricated a high sensitive paper-based sensor for cancer biomarker (carcinoembryonic antigen, CEA) detection by dip coating a PEDOT:PSS (Sigma Aldrich), EG (3.0 v/v), and rGO (0.035 w/w%) mixture. The PEDOT:PSS-rGO coated paper exhibited $S = 3.12 \times 10^{-2}$ S/cm, higher than the one of pure PEDOT:PSS coated paper, $S = 1.16 \times 10^{-4}$ S/cm. Moreover, in the presence of rGO, the charge transfer resistance (R_{ct}) decreased from 7.0 kΩ to 2.8 kΩ, and the electron transfer rate constant (K_{ct}) value, equal to $K_{ct} = 1.9 \times 10^{-5}$ cm/s, was 2.5 times higher than the one of PEDOT:PSS/EG coated paper. The use of rGO in PEDOT:PSS (Sigma Aldrich) was also investigate for glucose detection by Abd-Wahab et al. [132]. Particularly, after blending the composite with glucose oxidase, the sensitivity reached a peak of 57.3 μA/(mM·cm^2) and a detection limit of 86.8 μM. Interestingly, a structural change was detected when blending the PEDOT into the graphene, which generates a PEDOT:PSS matrix interspersed between rGO layers (see Fig. 6B, C). The final *S* increased, probably due to the formation of a π-π interaction between PEDOT and the rGO surface; electrochemical activity also enhanced from a peak current of 0.522 mA to 1.184 mA.

Alternatively, deposited PEDOT:PSS (Sigma Aldrich)/graphene nanoplatelets (GNPs) composites were electro-spraying deposited on fluorine-doped tin oxide (FTO) electrodes for the detection of dopamine (DA) in aqueous medium in the presence of ascorbic acid and uric acid [158]. The PEDOT:PSS-GNPs electrodes were treated with concentrated

H_2SO_4 (98 %) to remove the insulating and hydrophilic PSS from the composites. The final PEDOT:PSS-GNPs composites exhibited high stability in water, improved $S = 105.0$ S/cm and a low $R_{ct} = 54.8$ Ω at the electrode-electrolyte interface. Furthermore, the PEDOT:PSS-GNPs electrodes showed enhanced catalytic activity and sensitivity of DA in the presence of ascorbic acid and uric acid.

6.2. CNTs and their incorporation in PEDOT:PSS

CNTs are coaxial tubes formed from sp^2 carbon atoms with a small amount of sp^3 carbon atoms in the form of defects. CNTs can be considered as one dimensional (1D) nanocylinders rolled up from 2D graphene sheets [159]. A single graphitic layer or multiple coaxial layers can be rolled up into single-walled carbon nanotubes (SWCNTs) or multiwalled carbon nanotubes (MWCNTs), respectively [159]. CVD is the most common procedure for the synthesis of CNTs at a large scale production [127,160]. However, this method produces contaminants that can affect the properties of CNTs and often require expensive thermal annealing and/or chemical treatment for their removal [161]. Currently, the cheapest CNTs on the market, such as purified MWNTs, cost about $100/kg [160]. CNTs have been widely used in electronics due to their thermal conductivity (2800–6000 W/mK) [162], low electron scattering, and controlled band-gap [160]. They have been also used as electrodes or electrode coatings to record field potential and electrically stimulate cells [163] due to their electrocatalytic activity [83], high surface area (1315 m^2/g for SWCNTs) [164], mechanical flexibility, and electrical conductivity ($S = [10^6–10^7]$ S/m for pure CNTs) [165]. For instance, Gerwig et al. [166] electrodeposited a mixture of PEDOT:PSS and functionalized SWCNTs (P_2-SWCNTs) on the top of MEAs gold electrodes for the detection of primary cardiomyocytes activities. The biocompatible PEDOT:PSS-SWCNT composite exhibited a lower impedance and a 3× higher CIC than the control one based on TiN electrodes. Moreover, *CSC* enhanced from 0.45 ± 0.12 mC/cm^2 to 1.21 ± 0.02 mC/cm^2. Cardiomyocytes (HL-1 cells) activities were also detected by Zips et al. [167], by means of an aerosol jet printed MEA composed of a mixture of PEDOT:PSS (Sigma Aldrich), deionized water, glycerol, EG, GOPS, CMC and MWCNTs (final $S = 323 \pm 75$ S/m). The printed PEDOT:PSS-MWCNTs μ-needle electrodes showed a capacitance (*C*, nF) of 242 ± 70 nF at a scan rate of 5 mV/s and an impedance of 128 ± 22 kΩ at a frequency of 1 kHz.

Nevertheless, pristine CNTs are highly hydrophobic and aggregate in aqueous solution [168]. In addition, in the presence of oxygen they can damage DNA, alter cell cycle and cause cellular oxidative stress [169,170]. Therefore, in order to reduce their toxicity, their surface can be functionalized by oxidation and substitution or addition reactions, or by adsorption of proteins or lipids [133,171,172]. For instance, Wang et al. [173] electrodeposited a solution of PEDOT:PSS (0.1 w/w% EDOT, 0.2 w/w% PSS, Yacoo Corp, China) functionalized with MWCNTs-COOH (2.0 mg/mL) in deionized water, on nickel–cadmium (Ni–Ca) microwire electrodes. Afterwards, two peptides (Gly-Tyr-Ile-Gly-Ser-Arg, GYIGSR and Arg-Gly-Asp, RGD) were covalently bonded on the surface of the PEDOT:PSS-MWCNTs-COOH films in order to promote the neural cell adhesion, spreading and growth. The impedance of the final electrode decreased from $Z \sim 600$ kΩ to $Z = 15$ kΩ at 1 kHz, while the *CSC* increased 0.227 mC/cm^2 to 7.5032 mC/cm^2, compared to an unmodified Ni–Ca microwire electrode. Furthermore, PC12 cells were successfully cultured on the composite, and, in the presence of a neural growth factor (NGF), neurite extensions were detected.

Similarly to graphene, CNTs have been widely used in biosensors to improve electronic sensitivity. As an example, Wang et al. [83] studied the effect of SWCNTs (1.0 w/w%, volume ratio 8:1) and polyvinylpyrrolidone (PVP, 2.0 w/w%, volume ratio 9:1) as sensing electrocatalytic enhancer and stabilizer in a PEDOT:PSS aqueous solution (1.3 w/w%, Bayer AG) for the fabrication of film electrodes, able to detect eugenol in food samples. Due to a good soaking and conductive ability, the sensitivity detection showed a wide linear range till 122.4 μM and a low detection limit of 0.048 μM. The incorporation of PEDOT:PSS into a functionalized SWCNTs (SWCNT-COONa)-PVA network also increased *S*, due to the strong π–π interactions among the C═C bonds of SWCNTs and thiophene rings of PEDOT:PSS [174]. This composite was selected for the fabrication of a soft actuator for robotics and biomimetic applications, as a promising alternative to expensive Pt and Au actuators [175]. In details, the SWCNT-PVA-PEDOT:PSS membrane actuator showed good molecular rigidity (621.27 ± 5.34 MPa), high mechanical strength (28.8 ± 1.88 MPa), high $CSC = 0.00131$ F, and a low $R_{ct} = 4206.7$ Ω cm^2. Other unconventional biosensing applications include field effect transistors (FETs) [179], human motion monitoring sensors [180], and strain sensors [177,181].

The CNTs ability to enhance PEDOT:PSS conductivity found exploitation also for the fabrication of 2D and 3D bioengineered constructs in tissue engineering. For instance, Yen et al. [178] fabricated 2D conductive electrospun nanofibers using a solution of PEDOT:PSS (Clevios™ PH1000), MWCNTs (0.0–5.0 w/w%), poly(ethylene oxide) (PEO) at 15.0 w/w% and GOPS at 3.0 w/w%, for the development of hemodialysis devices. The nanofiber composite exhibited an enhanced $S \sim 1$ S/cm, with 3 w/w% of MWCNTs, compared to the pristine PEDOT:PSS-PEO nanofibers. Viability tests on human leukemic cells (THP1) also showed a viability higher than 90 %. 3D electroactive scaffold were instead prepared by Jayaram et al. [133], which freeze dried a PEDOT:PSS solution (Clevios™ PH1000), mixed with 0.5 w/w% DBSA, 3.0 w/w % GOPS, and MWCNTs (PEDOT:PSS/MWCNTs ratios equal to 1:1 and 2:3) (see Fig. 6D, E). The resulting 3D electrode exhibited a nanostructured porous morphology, a lower electrical resistance of about 7 times, and a lower impedance over the whole frequency spectra ($0.1–10^5$ Hz), compared to the neat PEDOT:PSS samples. Moreover, good cytocompatibility was verified by the spreading of telomerase-immortalized fibroblasts (TIFs) over the scaffold (up to 2 days).

7. Conclusion and future perspectives

In the field of bioelectronics, there is a growing demand for the exploration of new materials which meet several criteria, including cost-effectiveness, ease of processing, biocompatibility, conductivity, resistance to moisture, and adhesion to the substrate. Among these materials, PEDOT:PSS stands out as one of the most promising organic electroactive CPs. This popularity is attributed to its remarkable electrochemical and mechanical properties, as well as its biocompatibility with various cellular lineages. Additionally, PEDOT:PSS is commercially available at competitive prices, offering different PEDOT/PSS ratios that can be tailored to meet specific requirements. Its ease of processing and tunability further enhance its suitability for diverse bioelectronic applications, including the production of thin films, flexible/stretchable electrodes, sensors, coating materials, and scaffolds. Due to these exceptional properties, PEDOT:PSS the interest in PEDOT:PSS for bioelectronics significantly increased over the past few decades. PEDOT:PSS has been used in many emerging bioelectronic applications, including, wearable devices, 3D biomimetic interfaces for cellular activity stimulation, and also in-vivo bioelectronic devices. However, the development of PEDOT:PSS formulations that can effectively address the unique requirements of bioelectronics presents multiple challenges.

In this review, the authors provide an overview of various approaches for tailoring PEDOT:PSS properties for bioelectronics and TE. Particular emphasis is placed on achieving or ensuring: i) biocompatibility, ii) conductivity, iii) stability in saline solution, and iv) adhesion to the substrate. To the best of the authors' knowledge, this manuscript is the first attempt to provide a comprehensive overview of various methods for attaining these properties, while maintaining biocompatibility as priority. The review also gives some remarks with respect to the additional aspect of biodegradability, despite no viable biodegradable formulation is currently available.

Eventually, the last section presents a summary on the incorporation of carbon fillers into PEDOT:PSS mixtures, with a specific focus on

graphene and CNTs. Carbon-based fillers can indeed act as conductivity or specific properties enhancers.

Although significant progress has been made, there remains a significant amount of work to be done in the study of PEDOT:PSS. As reported by Boehler et al., the transition of PEDOT and its composites, including PEDOT:PSS, to a clinical validation (FDA approval in USA or CE mark in European economic area) still indeed remains a challenge [96]. This is mostly caused by the high versatility of the material, which is rather considered a material class, in which any new variation or alteration, including the production technique, dopant or additive used, must be analyzed to be fully validated and approved. Therefore, it is most likely that just only formulations targeted to a specific application will undergo clinical trials.

Furthermore, optimization on minimizing trade-offs among PEDOT:PSS properties, particularly when addressing the enhancement of conductivity and biodegradability, will be part of future researches. Accomplishing these goals will likely require modifications to the PEDOT:PSS formulation at the molecular backbone level. Additionally, more extensive research is needed on PEDOT:PSS biocompatibility, particularly in the context of long-term in vivo implantation, requiring long-term experimental campaigns.

To summarize, although the current scenario present some technical and regulatory challenges, PEDOT:PSS has showcased its promise, and its utilization is expected to increase in the coming years.

Credit authorship contribution statement

Conceptualization, M.S., E.F., and C.E.C.; methodology, M.S.; writing—original draft preparation, M.S. and A.G.; writing—review and editing, M.S., A.G., C.E.C and E.F.; visualization, M.S.; supervision, E.F.; project administration, E.F. . We thank Dr. Enrica Stasi (UniSalento, IT) for fruitful insights and discussions.

Funding

This research was funded by Research Foundation Flanders (FWO), with the doctoral fellowship granted to Miriam Seiti, number 1SB1120N.

Declaration of competing interest

The authors declare no conflict of interest.

Data availability

Data will be made available on request.

References

[1] L. Groenendaal, F. Jonas, D. Freitag, H. Pielartzik, J.R. Reynolds, Adv. Mater. 12 (7) (2000) 481–494.
[2] M. Seiti, P.S. Ginestra, E. Ceretti, E. Ferraris, A. Ranga, *Adv Mater* Interfaces 9 (2022) 1–21, 2101297.
[3] B. Liu, Y. Peng, Z. Jin, X. Wu, H. Gu, D. Wei, Y. Zhu, S. Zhuang, Chem. Eng. J. 462 (2023), 142347.
[4] Y. Zhang, X. Xiao, H. Feng, M.A. Nikitina, X. Zhang, Q. Zhao, Front Sustain Food Syst 7 (2023), 1172522.
[5] L. Wang, Y. Wu, T. Hu, B. Guo, P.X. Ma, Acta Biomater. 59 (2017) 68–81.
[6] A. Puiggalí-Jou, L.J. del Valle, C. Alemán, J. Control. Release 309 (2019) 244–264.
[7] D. Cherian, A. Armgarth, V. Beni, U. Linderhed, K. Tybrandt, D. Nilsson, D. T. Simon, M. Berggren, Flex Print Electron 4 (2) (2019), 022001.
[8] Y. Wen, J. Xu, J Polym Sci Part A Polym Chem 55 (7) (2017) 1121–1150.
[9] G. Huseynova, K.Y. Hyun, J.H. Lee, J. Lee, J Inf Disp 21 (2) (2020) 71–91.
[10] M. Uz, S.K. Mallapragada, J. Indian Inst. Sci. 99 (3) (2019) 489–510.
[11] F. Louwet, L. Groenendaal, J. Dhaen, J. Manca, J. Van Luppen, E. Verdonck, et al., Synth. Met. 135–136 (2003) 115–117.
[12] F. Jonas, L. Schrader, Synth. Met. 41 (3) (1991) 831–836.
[13] S. Kirchmeyer, K. Reuter, J. Mater. Chem. 15 (21) (2005) 2077–2088.
[14] A. Iyer, J. Hack, D.A.A. Trujillo, B. Tew, J. Zide, R. Opila, Appl. Sci. 8 (11) (2018) 1–12.
[15] B. Lu, H. Yuk, S. Lin, N. Jian, K. Qu, J. Xu, X. Zhao, Nat. Commun. 10 (2019) 1.
[16] D. Belaineh, J.W. Andreasen, J. Palisaitis, A. Malti, K. Håkansson, L. Wågberg, et al., ACS Appl Polym Mater 1 (9) (2019) 2342–2351.
[17] C.S. Park, C. Lee, O.S. Kwon, Polymers 8 (7) (2016) 1–18.
[18] Heraeus Epurio - CleviosTM™. https://www.heraeus.com/en/hep/products_hep/clevios/clevios_prod/clevios_1.html.
[19] Printed Conductors - Specialty Products. https://www.agfa.com/specialty-products/solutions/conductive-materials/printed-conductors/.
[20] H. Zhang, J. Xu, Y. Wen, Z. Wang, J. Zhang, W. Ding, Synth. Met. 204 (2015) 39–47.
[21] S. Zhang, P. Kumar, A.S. Nouas, L. Fontaine, H. Tang, F. Cicoira, APL Mater. 3 (2015) 1.
[22] Z. Wang, J. Xu, Y. Yao, L. Zhang, Y. Wen, H. Song, et al., Sensors Actuators, B Chem 196 (2014) 357–369.
[23] Z. Yu, Y. Xia, D. Du, J. Ouyang, ACS Appl. Mater. Interfaces 8 (35) (2016) 23204–23211.
[24] S. Lee, T. Eom, M.K. Kim, S.G. Yang, B.S. Shim, Electrochim. Acta 313 (2019) 79–90.
[25] A.G. Ulyashin, A. Hadjadj, M.A. Butt, Coatings 12 (2022) 1115.
[26] L. Hu, J. Song, X. Yin, Z. Su, Z. Li, Polymers 12 (2020) 1.
[27] M. Seiti, O. Degryse, E. Ferraris, Mater Today Proc 70 (2022) 38–44.
[28] Z. Xiong, C. Liu, Org. Electron. 13 (9) (2012) 1532–1540.
[29] M. Marzocchi, I. Gualandi, M. Calienni, I. Zironi, E. Scavetta, G. Castellani, et al., ACS Appl. Mater. Interfaces 7 (32) (2015) 17993–18003.
[30] T. Takano, H. Masunaga, A. Fujiwara, H. Okuzaki, T. Sasaki, Macromolecules 45 (9) (2012) 3859–3865.
[31] X. Fan, W. Nie, H. Tsai, N. Wang, H. Huang, Y. Cheng, et al., Adv. Sci. 6 (19) (2019), 1900813.
[32] M. Getnet Tadesse, C. Loghin, Y. Chen, L. Wang, D. Catalin, V. Nierstrasz, Smart Mater. Struct. 26 (6) (2017).
[33] A. Giuri, S. Colella, A. Listorti, A. Rizzo, C. Mele, C.E. Corcione, Compos. Part B Eng. 148 (2018) 149–155.
[34] A. Giuri, R. Striani, S. Carallo, S. Colella, A. Rizzo, C. Mele, et al., Electrochim. Acta 441 (2023), 141780.
[35] N. Gao, J. Yu, Q. Tian, J. Shi, M. Zhang, S. Chen, et al., Chemosens 9 (4) (2021) 79.
[36] B. Piro, G. Mattana, S. Zrig, G. Anquetin, N. Battaglini, D. Capitao, et al., Appl Sci 8 (2018) 6.
[37] F.P. Du, N.N. Cao, Y.F. Zhang, P. Fu, Y.G. Wu, Z.D. Lin, et al., Sci. Rep. 8 (1) (2018) 1–12.
[38] S.K. Kim, J.H. Mo, J.Y. Kim, K.S. Jang, E-Polymers 17 (6) (2017) 501–506.
[39] K.M. Reza, S. Mabrouk, Q. Qiao, Proc Nat Res Soc 2 (1) (2018) 68.
[40] H.Q. Cui, R.X. Peng, W. Song, J.F. Zhang, J.M. Huang, J.Q. Zhu, et al., Chinese J Polym Sci 37 (8) (2019) 760–766.
[41] Y. Sun, S. Yang, P. Du, F. Yan, J. Qu, Z. Zhu, et al., Opt. Express 25 (3) (2017) 1723.
[42] B.J. Worfolk, S.C. Andrews, S. Park, J. Reinspach, N. Liu, M.F. Toney, et al., Proc. Natl. Acad. Sci. 112 (46) (2015) 14138–14143.
[43] I. Song, N. Yeon Park, G. Seung Jeong, J. Hwan Kang, J. Hwa Seo, J.Y. Choi, Appl. Surf. Sci. 529 (2020), 147176.
[44] H.S. Kang, D.H. Kim, T.W. Kim, Sci. Rep. 11 (1) (2021) 1–9.
[45] J.P. Thomas, L. Zhao, D. McGillivray, K.T. Leung, J. Mater. Chem. A 2 (7) (2014) 2383–2389.
[46] X. Crispin, F.L.E. Jakobsson, A. Crispin, P.C.M. Grim, P. Andersson, A. Volodin, et al., Chem. Mater. 18 (18) (2006) 4354–4360.
[47] M. Solazzo, M.G. Monaghan, Biomater. Sci. 9 (2021) 4317–4328.
[48] G. Polino, C. Lubrano, P. Scognamiglio, V. Mollo, S. De Martino, G. Ciccone, et al., Flex Print Electron 5 (2020) 1.
[49] A. López, Conducting Polymer Materials for Bioelectronics Applications, University of the Basque Country UPV/EHU (Spain), 2018.
[50] M.M. De Kok, M. Buechel, S.I.E. Vulto, P. Van De Weyer, E.A. Meulenkamp, S.H.P. M. De Winter, A.J.G. Mank, H.J.M. Vorstenbosch, C.H.L. Weijtens, V. van Elsbergen, Phys Status Solidi Appl Res 201 (6) (2004) 1342–1359.
[51] Y. Han, Enhanced electrical properties of PEDOT:PSS via synergistic effect, Soft Mater. ISSN: 15394468 14 (2018) 2447–2453, https://doi.org/10.1080/1539445X.2017.1387151.
[52] T. Wang, Y. Qi, J. Xu, X. Hu, P. Chen, Appl. Surf. Sci. 250 (1–4) (2005) 188–194.
[53] X. Fan, Adv. Funct. Mater. 31 (8) (2021), 2009399.
[54] A. Elschner, S. Kirchmeyer, W. Lovenich, U. Merker U., PEDOT: Principles and Applications of an Intrinsically Conductive Polymer, CRC Press, USA, 2010.
[55] W. Jeong, G. Gwon, J.H. Ha, D. Kim, K.J. Eom, J.H. Park, et al., Biosens. Bioelectron. 171 (2021), 112717.
[56] J. Rivnay, S. Inal, B.A. Collins, M. Sessolo, E. Stavrinidou, X. Strakosas, et al., Nat. Commun. 7 (2016) 11287.
[57] H. Shi, C. Liu, Q. Jiang, J. Xu, Adv Electron Mater 1 (4) (2015) 1–16.
[58] S.P. Rwei, Y.H. Lee, J.W. Shiu, R. Sasikumar, U.T. Shyr, Polymers 11 (1) (2019) 134.
[59] Y. Xia, K. Sun, J. Ouyang, Energ. Environ. Sci. 5 (1) (2012) 5325–5332.
[60] N. Kim, S. Kee, S.H. Lee, B.H. Lee, Y.H. Kahng, Y.R. Jo, et al., Adv. Mater. 26 (14) (2014) 2268–2272.
[61] M. Seiti, P.S. Ginestra, R.M. Ferraro, S. Giliani, R.M. Vetrano, E. Ceretti, et al., Int J Bioprinting 8 (1) (2022) 504.
[62] Y. Xia, J. Ouyang, J. Mater. Chem. 21 (13) (2011) 4927–4936.
[63] P. D'Angelo, G. Tarabella, A. Romeo, S.L. Marasso, A. Verna, M. Cocuzza, et al., Materials 12 (1) (2019) 9.
[64] A. Soleimani-Gorgani, Adv. Nat. Sci. Nanosci. Nanotechnol. 9(2):aac2a0 (2018).

[65] W.S. MacGregor, Ann. N. Y. Acad. Sci. 141 (1) (1967) 3–12.
[66] I. Cruz-Cruz, M. Reyes-Reyes, M.A. Aguilar-Frutis, A.G. Rodriguez, R. López-Sandoval, Synth. Met. 160 (13–14) (2010) 1501–1506.
[67] J.T. Kim, J. Pyo, J. Rho, J.H. Ahn, J.H. Je, G. Margaritondo, ACS Macro Lett. 1 (3) (2012) 375–379.
[68] Y.H. Kim, C. Sachse, M.L. MacHala, C. May, L. Müller-Meskamp, K. Leo, Adv. Funct. Mater. 21 (6) (2011) 1076–1081.
[69] O.P. Dimitriev, D.A. Grinko, Y.V. Noskov, N.A. Ogurtsov, A.A. Pud, Synth. Met. 159 (21–22) (2009) 2237–2239.
[70] S. Han, F. Jiao, Z.U. Khan, J. Edberg, S. Fabiano, X. Crispin, Adv. Funct. Mater. 27 (44) (2017) 1703549.
[71] H. Yue, Y. Zhao, X. Ma, J. Gong, Chem. Soc. Rev. 41 (11) (2012) 4218–4244.
[72] S. Stříteský, A. Marková, J. Víteček, E. Šafaříková, M. Hrabal, L. Kubáč, et al., J Biomed Mater Res - Part A 106 (4) (2018) 1121–1128.
[73] R. Christoph, B. Schmidt, U. Steinberner, W. Dilla, R. Karinen, Ullmann's Encycl Ind Chem (2006) 1–16.
[74] J.F. Li, C. Zhao, H. Zhang, et al., Chinese Phys B 25 (2) (2015), 028402.
[75] M.R. Moraes, A.C. Alves, F. Toptan, M.S. Martins, E.M.F. Vieira, A.J. Paleo, et al., J Mater Chem C 5 (2017) 3807.
[76] L.D. Garma, L.M. Ferrari, P. Scognamiglio, F. Greco, F. Santoro, Lab Chip 19 (22) (2019) 3776–3786.
[77] S. Tsukada, H. Nakashima, K. Torimitsu, PloS One 7 (4) (2012), e33689.
[78] W. Yin, E. Ruckenstein, Synth. Met. 108 (1) (2000) 39–46.
[79] S. Inal, A. Hama, M. Ferro, C. Pitsalidis, J. Oziat, D. Iandolo, et al., Adv Biosyst 1 (6) (2017) 1–9.
[80] Y. Li, X. Li, S. Zhang, L. Liu, N. Hamad, S.R. Bobbara, et al., Adv. Funct. Mater. 30 (30) (2020) 1–9.
[81] Y. Liu, A.F. McGuire, H.Y. Lou, T.L. Li, J.B.H. Tok, B. Cui, et al., Proc. Natl. Acad. Sci. U. S. A. 115 (46) (2018) 11718–11723.
[82] M. Solazzo, K. Krukiewicz, A. Zhussupbekova, K. Fleischer, M.J. Biggs, M. G. Monaghan, J. Mater. Chem. B 7 (31) (2019) 4811–4820.
[83] Z. Wang, Y. Yao, H. Zhang, J. Zhang, W. Ding, Z. Liu, et al., Int. J. Electrochem. Sci. 10 (9) (2015) 6997–7012.
[84] A. Håkansson, S. Han, S. Wang, J. Lu, S. Braun, M. Fahlman, et al., J Polym Sci Part B 55 (10) (2017) 814–820.
[85] M. Vázquez, P. Danielsson, J. Bobacka, A. Lewenstam, A. Ivaska, Sens. Actuators B 97 (2–3) (2004) 182–189.
[86] J. Huang, P.F. Miller, J.S. Wilson, A.J. De Mello, J.C. De Mello, D.D.C. Bradley, Adv. Funct. Mater. 15 (2) (2005) 290–296.
[87] D. Mantione, I. Del Agua, W. Schaafsma, M. Elmahmoudy, I. Uguz, A. Sanchez-Sanchez, et al., ACS Appl. Mater. Interfaces 9 (21) (2017) 18254–18262.
[88] M. ElMahmoudy, S. Inal, A. Charrier, I. Uguz, G.G. Malliaras, S. Sanaur, Macromol. Mater. Eng. 302 (5) (2017) 1–8.
[89] G. Dijk, A.L. Rutz, G.G. Malliaras, Adv Mater Technol 5 (2020) 3.
[90] A.G. Guex, J.L. Puetzer, A. Armgarth, E. Littmann, E. Stavrinidou, E.P. Giannelis, et al., Acta Biomater. 62 (2017) 91–101.
[91] D. Shao, H. Zhong, L. Zhang, ChemElectroChem 1 (10) (2014) 1679–1687.
[92] M.A. Kamenskii, A.I. Vypritskaya, S.N. Eliseeva, A.I. Volkov, V.V. Kondratiev, Mater. Lett. 282 (2021), 128658.
[93] T.W. Kwon, J.W. Choi, A. Coskun, Chem. Soc. Rev. 47 (6) (2018) 2145–2164.
[94] M.J. Donahue, A. Sanchez-Sanchez, S. Inal, J. Qu, R.M. Owens, D. Mecerreyes, et al., Mater Sci Eng R Reports 140 (2020), 100546.
[95] S. Zhang, E. Hubis, C. Girard, P. Kumar, J. DeFranco, F. Cicoira, J. Mater. Chem. C 4 (7) (2016) 1382–1385.
[96] C. Boehler, Z. Aqrawe, M. Asplund, Bioelectron Med 2 (2) (2019) 89–99.
[97] L.V. Kayser, D.J. Lipomi, Adv. Mater. 31 (10) (2019) 1–13.
[98] Y. Lu, Y. Li, J. Pan, P. Wei, N. Liu, B. Wu, et al., Biomaterials 33 (2) (2012) 378–394.
[99] M. Berggren, A. Richter-Dahlfors, Adv. Mater. 19 (20) (2007) 3201–3213.
[100] K. Feron, R. Lim, C. Sherwood, A. Keynes, A. Brichta, P.C. Dastoor, Int. J. Mol. Sci. 19 (8) (2018) 2382.
[101] A.M. Pappa, H.Y. Liu, W. Traberg-Christensen, Q. Thiburce, A. Savva, A. Pavia, A. Salleo, S. Daniel, R.M. Owens, ACS Nano 6 (2020) 8.
[102] Y. Liang, A. Offenhäusser, S. Ingebrandt, D. Mayer, Adv. Healthc. Mater. 10 (11) (2021), 2100061.
[103] J.E. McCarthy, C.A. Hanley, L.J. Brennan, V.G. Lambertini, Y.K. Gun'Ko, J Mater Chem C 2 (4) (2013) 764–770.
[104] X. Fan, N.E. Stott, J. Zeng, Y. Li, J. Ouyang, L. Chu, W. Song, J. Mater. Chem. A 11 (2023) 18561–18591.
[105] J. Song, G. Ma, F. Qin, L. Hu, B. Luo, T. Liu, X. Yin, Z. Su, Z. Zeng, Y. Jiang, G. Wang, Z. Li, Polymers 12 (2020) 2.
[106] A.M.D. Wan, S. Inal, T. Williams, K. Wang, P. Leleux, L. Estevez, et al., J. Mater. Chem. B 3 (25) (2015) 5040–5048.
[107] X. Strakosas, M. Sessolo, A. Hama, J. Rivnay, E. Stavrinidou, G.G. Malliaras, et al., J. Mater. Chem. B 2 (17) (2014) 2537–2545.
[108] D. Marrero, A. Guimera, L. Maes, R. Villa, M. Alvarez, X. Illa, Lab Chip 23 (7) (2023) 1825–1834.
[109] Y.S. Hsiao, E.D. Quiñones, S.C. Yen, J. Yu, J.T. Fang, P. Chen, R.S. Juang, ACS Appl. Mater. Interfaces 15 (18) (2023) 21953–21964.
[110] D. Won, J. Kim, J. Choi, H.J. Kim, S. Han, I. Ha, et al., Sci. Adv. 8 (23) (2022) 3209.
[111] Y. Furukawa, A. Shimada, K. Kato, H. Iwata, K. Torimitsu, Biochim Biophys Acta - Gen Subj 1830 (9) (2013) 4329–4333.
[112] L. Ferlauto, A.N. D'Angelo, P. Vagni, M.J.I.A. Leccardi, F.M. Mor, E.A. Cuttaz, et al., Front. Neurosci. 12 (2018) 648.
[113] S. Khan, S. Ali, A. Khan, B. Wang, A. Bermak, IEEE Sensors J. 21 (4) (2021) 4167–4175.
[114] A. Blau, A. Murr, S. Wolff, E. Sernagor, P. Medini, G. Iurilli, et al., Biomaterials 32 (7) (2011) 1778–1786.
[115] F. Hempel, J.K.Y. Law, T.C. Nguyen, W. Munief, X. Lu, V. Pachauri, et al., Biosens. Bioelectron. 93 (2017) 132–138.
[116] Y. Zheng, Y. Wang, F. Zhang, S. Zhang, K.D. Piatkevich, N. Zhou, et al., Adv Mater Technol 7 (7) (2022), 2101514.
[117] F. Pires, Q. Ferreira, C.A.V. Rodrigues, J. Morgado, F.C. Ferreira, Biochim Biophys Acta - Gen Subj 1850 (6) (2015) 1158–1168.
[118] M. Ganji, E. Kaestner, J. Hermiz, N. Rogers, A. Tanaka, D. Cleary, et al., Adv. Funct. Mater. 28 (2018) 12.
[119] M. Han, E. Yildiz, H.N. Kaleli, S. Karaz, G.O. Eren, I.B. Dogru-Yukse, et al., Adv. Healthc. Mater. 11 (8) (2022), 2102160.
[120] F. Amorini, I. Zironi, M. Marzocchi, I. Gualandi, M. Calienni, T. Cramer, et al., ACS Appl. Mater. Interfaces 9 (8) (2017) 6679–6689.
[121] X. Peng, K. Dong, Z. Wu, J. Wang, Z.L. Wang, J. Mater. Sci. 56 (30) (2021) 16765–16789.
[122] D.H. Lee, T. Park, H. Yoo, Polym 14 (2022) 2875.
[123] C. Boehler, Z. Aqrawe, M. Asplund, Bioelec in Med 2 (2019) 2.
[124] P. Ren, J. Dong, Adv Mater Technol 8 (17) (2023), 2300410.
[125] A. Zhuang, X. Huang, S. Fan, X. Yao, B. Zhu, Y. Zhang, ACS Appl. Mater. Interfaces 14 (1) (2022) 123–137.
[126] C. Wang, K. Xia, H. Wang, X. Liang, Z. Yin, Y. Zhang, Adv. Mater. 31 (2019), 1801072.
[127] S.K. Rastogi, A. Kalmykov, N. Johnson, T. Cohen-Karni, J. Mater. Chem. B 6 (2018) 7159–7178.
[128] G. Kaur, R. Adhikari, P. Cass, M. Bown, P. Gunatillake, RSC Adv. 5 (2015) 37553–37567.
[129] P.C. Mahakul, K. Sa, B. Das, B.V.R.S. Subramaniam, S. Saha, B. Moharana, et al., J. Mater. Sci. 52 (10) (2017) 5696–5707.
[130] P.J. Brigandi, J.M. Cogen, R.A. Pearson, Polym. Eng. Sci. 57 (12) (2014) 1329–1339.
[131] D. Untereker, S. Lyu, J. Schley, G. Martinez, L. Lohstreter, ACS Appl. Mater. Interfaces 1 (1) (2009) 97–101.
[132] F. Abd-Wahab, H.F.A. Guthoos, W.W.A. Wan Salim, Biosensors 9 (1) (2019).
[133] A.K. Jayaram, C. Pitsalidis, E. Tan, C.M. Moysidou, M.F.L. De Volder, J.S. Kim, et al., Front. Chem. (2019) 7.
[134] A. Rifai, E. Pirogova, K. Fox, Encyclopedia of Biomedical Engineering, Elsevier, USA, 2018, pp. 1–11.
[135] C. Fang, J. Zhang, X. Chen, G.J. Weng, Nanomaterials 10 (6) (2020) 1129.
[136] S. Zhang, H. Wang, J. Liu, C. Bao, Mater. Lett. 261 (2020), 127098.
[137] R. Mertens, NanoXplore. https://www.graphene-info.com/nanoxplore-plans-10000-ton-graphene-powder-facility. (Accessed April 2023).
[138] S. Park, R.S. Ruoff, Nat. Nanotechnol. 4 (2009) 217–224.
[139] C. Berger, Z. Song, X. Li, X. Wu, N. Brown, C. Naud, et al., Science 312 (5777) (2006) 1191–1196.
[140] X. Li, W. Cai, J. An, S. Kim, J. Nah, D. Yang, et al., Science 5;324(5932):1312-4 (2009).
[141] V.C. Sanchez, A. Jachak, R.H. Hurt, A.B. Kane, Chem. Res. Toxicol. 25 (1) (2012) 15–34.
[142] S.K. Rastogi, G. Raghavan, G. Yang, T. Cohen-Karni, Nano Lett. 17 (5) (2017) 3297–3301.
[143] A. Sasidharan, L.S. Panchakarla, P. Chandran, D. Menon, S. Nair, C.N.R. Rao, et al., Nanoscale 3 (2011) 2461–2464.
[144] A. Sasidharan, L.S. Panchakarla, A.R. Sadanandan, A. Ashokan, P. Chandran, C. M. Girish, et al., Small 8 (8) (2012) 1251–1263.
[145] Y. Zhang, T.R. Nayak, H. Hong, W. Cai, Nanoscale 4 (13) (2012) 3833–3842.
[146] Z. Guo, S. Chakraborty, A. Monikh, D.D. Varsou, A.J. Chetwynd, A. Afantitis, I. Lynch, P. Zhanget, Adv Biol 5 (9) (2021), 2100637.
[147] Y. Xu, K. Sheng, C. Li, G. Shi, ACS Nano 4 (7) (2010) 4324–4330.
[148] B.G. Choi, M. Yang, W.H. Hong, J.W. Choi, Y.S. Huh, ACS Nano 6 (5) (2012) 4020–4028.
[149] J. Lin, Z. Peng, Y. Liu, F. Ruiz-Zepeda, R. Ye, E.L.G. Samuel, et al., Nat. Commun. 5 (2014) 5714.
[150] N. Li, Q. Zhang, S. Gao, Q. Song, R. Huang, L. Wang, et al., Sci. Rep. 3 (2013) 1–6.
[151] L. Chen, L. Guo, Y. Wu, Y. Jia, Z. Li, X. Chen, RSC Adv. 3 (2013) 13926–13933.
[152] C. Yang, H. Bi, D. Wan, F. Huang, X. Xie, M. Jiang, J. Mater. Chem. A 1 (2013) 770–775.
[153] R. Garg, S.K. Rastogi, M. Lamparski, S.C. De La Barrera, G.T. Pace, N.T. Nuhfer, et al., ACS Nano 11 (6) (2017) 6301–6311.
[154] R. Ion, S. Vizireanu, C.E. Stancu, C. Luculescu, A. Cimpean, G. Dinescu, Mater. Sci. Eng. C 48 (2015) 118–125.
[155] P. Kshirsagar, S. Dickreuter, M. Mierzejewski, C.J. Burkhardt, T. Chassé, M. Fleischer, et al., Adv Mater Technol 4 (1) (2019), 1800318.
[156] L.A. Mercante, M.H.M. Facure, R.C. Sanfelice, F.L. Migliorini, L.H.C. Mattoso, D. S. Correa, Appl. Surf. Sci. 407 (2017) 162–170.
[157] S. Kumar, S. Kumar, S. Srivastava, B.K. Yadav, S.H. Lee, J.G. Sharma, et al., Biosens. Bioelectron. 73 (2015) 114–122.
[158] D. Liu, M.M. Rahman, C. Ge, J. Kim, J.J. Lee, New J. Chem. 41 (24) (2017) 15458–15465.
[159] Q. Xin, H. Shah, A. Nawaz, W. Xie, M.Z. Akram, A. Batool, et al., Adv. Mater. 31 (45) (2019), e1804838.
[160] M.F.L. De Volder, S.H. Tawfick, R.H. Baughman, A.J. Hart, Science 339 (6119) (2013) 535–539.

[161] J. Prasek, J. Drbohlavova, J. Chomoucka, J. Hubalek, O. Jasek, V. Adam, et al., J. Mater. Chem. 21 (2011) 15872–15884.
[162] Z. Han Z, A. Fina., Prog. Polym. Sci. 36 (70) (2011) 914–944.
[163] L.B. Keren, Y. Hanein, Front, Neural Circuits (2012) 6.
[164] M.E. Birch, T.A. Ruda-Eberenz, M. Chai, R. Andrews, R.L. Hatfield, Ann. Occup. Hyg. 57 (9) (2013) 1148–1166.
[165] Y. Wang, G.J. Weng, Micromechanics and Nanomechanics of Composite Solids, Springer International Publishing, New York, USA, 2017.
[166] R. Gerwig, K. Fuchsberger, B. Schroeppel, G.S. Link, G. Heusel, U. Kraushaar, et al., Front Neuroeng 5 (2012) 1–11.
[167] S. Zips, L. Grob, P. Rinklin, K. Terkan, N.Y. Adly, L.J.K. Weiß, et al., ACS Appl. Mater. Interfaces 11 (36) (2019) 32778–32786.
[168] A. Bianco, K. Kostarelos, M. Prato, Curr. Opin. Chem. Biol. 9 (6) (2005) 674–679.
[169] G. Hong, S. Diao, A.L. Antaris, H. Dai, Chem. Rev. 115 (19) (2015) 10816–10906.
[170] C.P. Firme, P.R. Bandaru, Biol. Med. 6 (2) (2010) 245–256.
[171] C.M. Sayes, F. Liang, J.L. Hudson, J. Mendez, W. Guo, J.M. Beach, et al., Toxicol. Lett. 161 (2) (2005) 135–142.
[172] G. Jin, K. Li, Mater. Sci. Eng. C 45 (2015) 671–681.
[173] K. Wang, R.Y. Tang, X.B. Zhao, J.J. Li, Y.R. Lang, X.X. Jiang, et al., Nanoscale 7 (2015) 18677–18685.
[174] R. Jalili, J.M. Razal, G.G. Wallace, Sci. Rep. 3 (2013) 3438.
[175] A. Khan, R.K. Jain, P. Banerjee, K.A. Alamry, B. Ghosh, Inamuddin, et al., J. Reinf. Plast. Compos. 40 (3–4) (2021).
[176] K. Wang, L. Tian, T. Wang, Z. Zhang, X. Gao, L. Wu, et al., Compos Interfaces 26 (1) (2019) 27–40.
[177] G. Tadayyon, K. Krukiewicz, J. Britton, A. Larrañaga, C. Vallejo-Giraldo, M. Fernandez-Yague, et al., Mater. Sci. Eng. C 121 (2021), 111857.
[178] S.C. Yen, Z.W. Liu, R.S. Juang, S. Sahoo, C.H. Huang, P. Chen, et al., ACS Appl. Mater. Interfaces 11 (47) (2019) 43843–43856.
[179] F. Molina-Lopez, T.Z. Gao, U. Kraft, C. Zhu, T. Öhlund, R. Pfattner, et al., Nat. Commun. 10 (1) (2019) 1–10.
[180] Z. Zhao, X. Yuan, Y. Huang, J. Wang, New J. Chem. 45 (2021) 208–216.
[181] F. Jabbar, A.M. Soomro, J.W. Lee, M. Ali, Y. Su Kim, S.H. Lee, et al., Sensors Mater 32 (12) (2020) 1–17.

Miriam Seiti is pursuing a Dual Ph.D. in Engineering Technology at KU Leuven (BE) and Ph.D. in Mechanical and Industrial Engineering at University of Brescia (IT), in collaboration with Nerf (Imec, BE), since 2019. She holds a Fonds Wetenschappelijk Onderzoek (FWO) strategic research fellowship. Her research involves the use of additive manufacturing techniques for neural tissue engineering and bioelectronics. She earned a Bachelor's and Master's degree in Management and Industrial Engineering from University of Brescia (Italy), both 110/100 cum laude, respectively in 2016 and 2019.

Antonella Giuri received her Ph.D in Materials and Structure Engineering and Nanotechnology in 2019 from University of Salento. During her Ph.D, she joined the group of Prof. Feng Gao (University of Linköping, Sweden) and the group of Prof. Cristopher Tuck (CfAM, Nottingham University, UK), working on the implementation and on the scalability of the developed polymer-perovskite composite. From 2019 to now she worked as postdoctoral fellow at the CNR-Nanotec in Lecce with Dr. Aurora Rizzo. Her research interest focuses on nanocomposites materials for energy conversion.

Carola Esposito Corcione received her Ph.D. degree in Materials Science and Technology in May 2004, from University of Salento (Italy). From January 2005 she is Associate Professor at University of Salento. Her research interest focuses on the rheological, thermal and transport properties of innovative polymeric materials, particularly polymer based nanocomposites, bio-polymers, largely employed in industrial applications (such as coatings, solar energy materials, automotive, medical, additive manufacturing, circular economy, reuse and recycle) focusing on the relationship between processing, structure and properties. She is author of about 150 papers on international journals, 100 presentations at international conferences and 4 patents (h_{index} 36).

Eleonora Ferraris is currently an Associate Professor of the Faculty of Engineering Technology, Department of Mechanical Engineering, KU Leuven, Belgium. She is responsible for research and teaching activities in the field of advanced manufacturing and she is head of the Advanced Manufacturing research Laboratory (AML), at Campus De Nayer. Her recent research activities focuses on nozzle based additive manufacturing, including extrusion and jet based printing for mechatronics and regenerative medicine. Ferraris received her PhD Degree in Material Engineering from University Tor Vergata of Rome in 2006, and her Master Degree in Industrial Engineering from Politecnico di Milano in 2002.